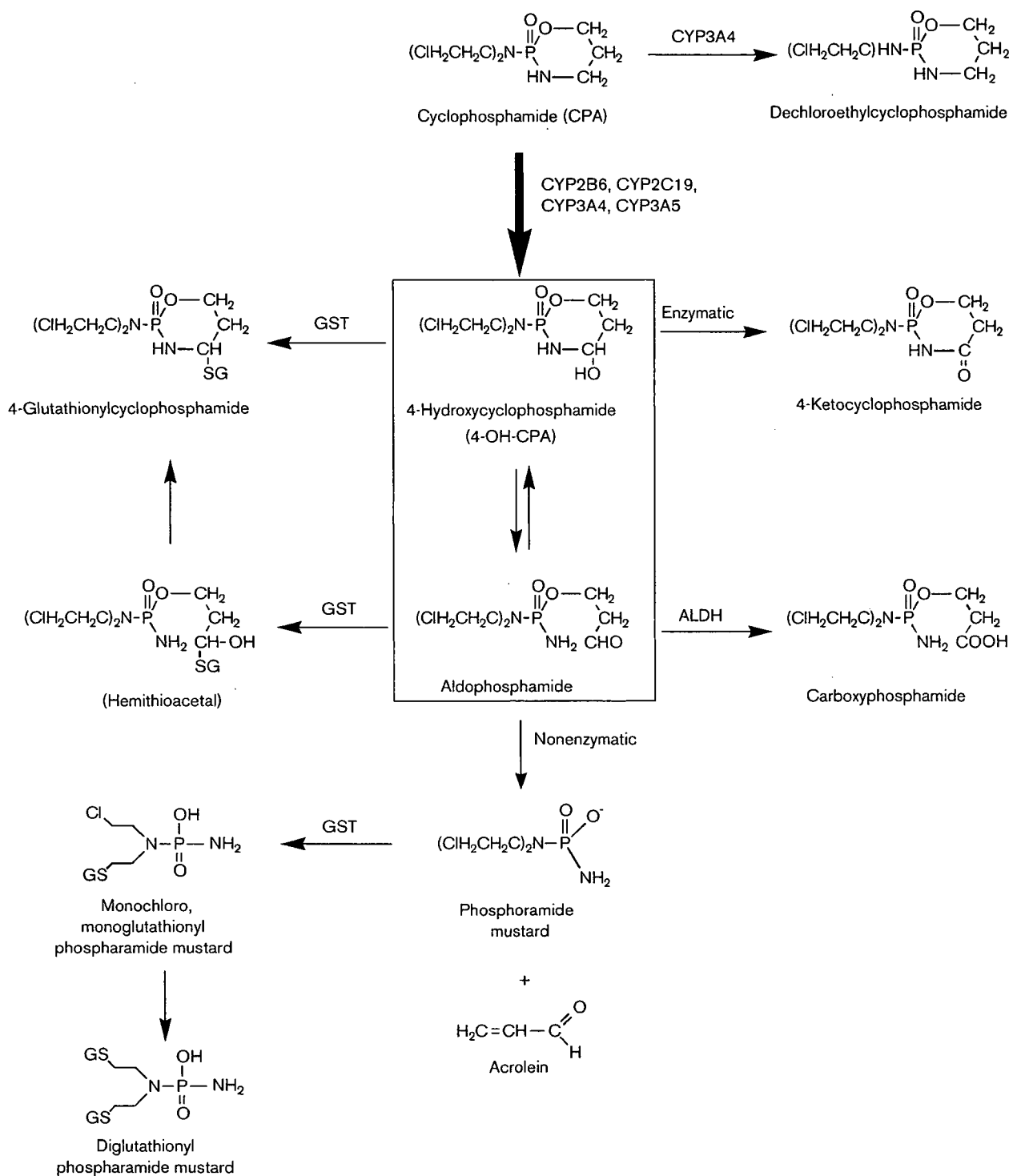Fig. 1

Activation and inactivation pathways of cyclophosphamide (CPA) in humans.

The drug-metabolizing enzymes described above are known to be highly polymorphic and have variant alleles with decreased or absent metabolic activity, resulting in large interindividual variability in the plasma concentrations of drugs. For *CYP2B6* gene, Lang *et al.* [9] first identified nine single nucleotide polymorphisms (SNPs),

of which five result in amino acid substitutions; *CYP2B6*2* (R22C), *CYP2B6*3* (S259R), *CYP2B6*4* (K262R), *CYP2B6*5* (R487C), *CYP2B6*6* (Q172H and K262R), and *CYP2B6*7* (Q172H, K262R, and R487C). Thereafter, Lamba et al. [10] reported *CYP2B6*8* (K139E) and *CYP2B6*9* (Q172H). Lang et al. [11] reported *CYP2B6*10* (Q21L and R22C), *CYP2B6*11* (M46V), *CYP2B6*12* (G99E), *CYP2B6*13* (K139E, Q172H, and K262R), *CYP2B6*14* (R140Q), and *CYP2B6*15* (I391N). Furthermore, several additional SNPs have been identified [12,13]. It has been reported that the amino acid change of R487C was associated with decreased CYP2B6 expression [9,10]. The amino acid change of Q172H [14] and K262R [15,16] has been reported to increase CYP2B6 activity. The *CYP2B6*6* having both substitutions, however, has been reported to be associated with the decreased expression and activity in liver [9,12], whereas heterologously expressed CYP2B6.6 revealed higher activity than that of the wild type [16]. Lang et al. [11] reported that *CYP2B6*8*, *CYP2B6*11*, *CYP2B6*12*, *CYP2B6*14*, and *CYP2B6*15* reduced the expression and/or function in heterologous expression system.

The side effects and clinical efficacy of CPA exhibit large interindividual variability, which might be because of differences in the pharmacokinetics. A few studies are available to investigate the relationship between the genetic polymorphisms of CYPs and pharmacokinetics of CPA. Xie et al. [17,18] have reported that *CYP2B6* variant causing the amino acid change Q172H, but not *CYP2C9* or *CYP2C19* variants, is associated with the increased CPA 4-hydroxylation. In contrast, Timm et al. [19] have reported that *CYP2C19*2* carriers had lowered elimination constants of CPA, whereas there was no association between *CYP2B6*, *CYP2C9*, and *CYP3A5* genotypes. In addition, Takada et al. [20] have reported that *CYP2C19*2*, but not *CYP2B6*, *CYP2C9*, or *CYP3A5* polymorphisms, is associated with a lower risk of developing premature ovarian failure, the most common long-term adverse effect of pulse CPA for treatment of severe lupus nephritis. These conflicting reports prompted us to investigate the relationship between the genetic polymorphisms of the enzymes and the pharmacokinetics and CPA in Japanese cancer patients. In this study, 103 Japanese patients with malignant lymphoma or breast cancer were investigated for the pharmacokinetics of CPA and 4-OH-CPA as well as the genetic polymorphisms of the *CYP2B6*, *CYP2C19*, *CYP3A4*, *CYP3A5*, *ALDH1A1*, and *GST* genes.

Materials and methods
Chemicals and reagents
CPA monohydrate, semicarbazide hydrochloride, hydroxylamine, and *m*-aminophenol were from Wako Pure Chemicals (Tokyo, Japan). 4-Hydroperoxycyclophospha-

mide (4-OOH-CPA) was kindly provided by Shionogi Pharmaceutical (Osaka, Japan). 5-Ethyl-5-*p*-tolylbarbituric acid (ETBA) was from Sigma Aldrich (St Louis, Missouri, USA). The Puregene DNA isolation kit was from Gentra Systems (Minneapolis, Minnesota, USA). Taq DNA polymerase and Ex Taq DNA polymerase were from Greiner Japan (Tokyo, Japan) and Takara (Shiga, Japan), respectively. Restriction enzymes were purchased from TOYOBO (Osaka, Japan), Takara, or New England Biolabs (Beverly, Massachusetts, USA). Primers were commercially synthesized at Hokkaido System Sciences (Sapporo, Japan). All other reagents were of the highest grade commercially available.

Patients, drug administration, and blood collection
This study was approved by the Ethics Committees of National Cancer Center Hospital East and Kanazawa University. Written informed consent was obtained from 103 Japanese patients (26 men and 77 women). Eligible patients were ≥ 20 years of age with histologically or cytologically confirmed malignant lymphoma ($n = 52$) or breast cancer ($n = 51$) and had never received prior treatments. Patients had to have a predicted life expectancy of ≥ 12 weeks. The inclusion/exclusion criteria consisted of the following: absolute neutrophil count $\geq 1200/\mu l$; absolute platelet count $\geq 75\,000/\mu l$; aspartate aminotransferase, alanine aminotransferase, and serum creatinine ≤ 2.5 times the upper limits of normal; total bilirubin ≤ 2 times the upper limits of normal; no severe concomitant disease. These patients were scheduled to receive the CHOP regimen [CPA, 500–750 mg/m^2, intravenously (i.v.); doxorubicin, 50 mg/m^2, i.v.; vincristine, 1.4 mg/m^2, i.v.; prednisolone, 100 mg/day, orally] ($n = 33$), R-CHOP regimen (CHOP with rituximab, 375 mg/m^2, i.v.) ($n = 19$) or AC regimen (doxorubicin, 60 mg/m^2, i.v.; CPA, 500–600 mg/m^2, i.v.) ($n = 51$). CPA (Endoxan, Shionogi, Osaka, Japan) was administered as a 1-h intravenous infusion. At first cycle of chemotherapy, blood samples (2 ml) were obtained from a cubital vein opposite the infusion site, before the infusion of CPA, at the middle, and the end of infusion, and 0.5, 1, 2, 3, 5, 7, 10, and 24 h after the end of the infusion. Immediately after collection in heparin tubes, the whole blood samples were placed on ice. An aliquot (1 ml) of the heparinized blood was centrifuged at 1500*g* for 3 min at 4°C to separate the plasma for the analysis of CPA. For the analysis of 4-OH-CPA, an aliquot (500 μl) of heparinized blood was immediately mixed with 5 μl of 0.5 mol/l semicarbazide to stabilize the metabolite [21], followed by centrifugation at 16 000*g* for 4 min. The separated plasma was stored at − 80°C until the analyses. Residual blood samples were used for the extraction of genomic DNA.

Determination of plasma concentration of cyclophosphamide
To 0.1 ml plasma samples, 0.9 ml of distilled water and 10 μl of ETBA (1.5 μg/ml) as an internal standard were

added. The mixture was extracted with 4 ml of dichloromethane by shaking for 10 min. The organic fraction was transferred to a clean tube and evaporated under a gentle stream of nitrogen at 40°C. The residue was redissolved in 100 μl of mobile phase and a portion of the 50 μl was injected into the high-performance liquid chromatography (HPLC). HPLC analysis was performed using a PU-980 intelligent HPLC pump (Jasco, Tokyo, Japan), a PU-970 intelligent UV/VIS detector (Jasco), an AS-950-10 intelligent sampler (Jasco), a D-2500 chromato-integrator (Hitachi, Tokyo, Japan), and a CTO-6A column oven (Shimadzu, Kyoto, Japan) with a Mightysil RP-18 GP Aqua column (150 × 4.6 mm, 5 μm; Kanto Chemical, Tokyo, Japan). The flow rate was 1.0 ml/min and the column temperature was 35°C. The eluate was monitored at 200 nm. The mobile phases were 30% CH_3CN/2 mmol/l KH_2PO_4 (pH 4.0). The retention times of CPA and ETBA were 5.4 and 9.8 min, respectively. None of the chromatograms showed any interfering peaks with CPA. Standard concentration curves were obtained from drug-free plasma added with known amounts of CPA in the range of 0–200 μmol/l. The quantification limit of CPA was 2 μmol/l.

Determination of plasma concentration of 4-hydroxy-cyclophosphamide

For quantification of 4-OH-CPA, an indirect fluorometric method measuring acrolein through the reaction with *m*-aminophenol in an acid media [1,6,22] was used. This assay involves acidic decomposition to acrolein, and condensation with *m*-aminophenol to yield 7-hydroxyquinoline, a fluorescent compound. To 60 μl plasma samples, 24 μl of 5.5% (w/v) zinc sulfate, 24 μl of saturated barium hydroxide, and 12 μl of 0.01 mol/l hydrochloric acid were added to precipitate the protein. After centrifugation at 15 000g for 15 min, 75 μl of the supernatant was added to 40 μl of a solution containing 6 mg/ml of 3-aminophenol and 6 mg/ml of hydroxylamine hydrochloride dissolved in freshly prepared 1 mol/l hydrochloric acid. The samples were heated at 90°C for 30 min in the dark and then allowed to cool to room temperature. An aliquot (50 μl) of the sample was subjected to HPLC. HPLC analysis was performed using an L-7100 pump (Hitachi), an L-7200 autosampler (Hitachi), a D-2500 Chromato-integrator (Hitachi), and a L7300 column oven (Hitachi) with a Mightysil RP-18 GP column (150 × 4.6-mm, 5 μm, Kanto Chemical). The eluent was monitored using a Hitachi L-7485 fluorescence detector (excitation, 350 nm; emission, 515 nm). The flow rate was 1.0 ml/min and the column temperature was 35°C. The mobile phase was 5% CH_3CN/0.1% H_3PO_4 (v/v). The retention time of 7-hydroxyquinoline was 3.5 min. For the preparation of a standard curve, 4-OOH-CPA was used as a substitute for 4-OH-CPA. In aqueous solution, 4-OOH-CPA liberates 4-OH-CPA/aldophosphamide. To the stock solution of 10 mmol/l 4-OOH-CPA, semicarbazide was added to a final concentration of 5 mmol/l. Standard concentration curves were obtained from drug-free plasma added with known amounts of stabilized 4-OOH-CPA in the range of 0–1.5 μmol/l. The detection limit of the plasma concentration of 4-OH-CPA was 0.07 μmol/l.

Pharmacokinetic analysis

The pharmacokinetics of CPA was evaluated by the model-dependent method with nonlinear mixed effect model [23]. The plasma concentration–time data were fitted to a two-compartment model using a zero-order infusion input. The total plasma clearance (CL) of CPA was calculated by multiplying the elimination rate constant (k_e), and distribution volume (V_d). The areas under the plasma concentration time curve (AUC) were calculated by dividing the dose by CL. The half-life $(t_{1/2})$ was calculated from $t_{1/2} = \ln 2/k_e$. The pharmacokinetics of 4-OH-CPA were evaluated by a moment analysis. AUC values were obtained using the trapezoidal rule and extrapolation to infinity by linear regression.

Analyses of genetic polymorphisms of CYP2B6 gene

Genomic DNA was extracted using the Puregene DNA isolation kit. *CYP2B6*4* (K262R), *CYP2B6*5* (R487C), *CYP2B6*6* (Q172H, K262R), *CYP2B6*7* (Q172H, K262R, R487C), *CYP2B6*8* (K139E), *CYP2B6*9* (Q172H), *CYP2B6*11* (M46V), *CYP2B6*12* (G99E), *CYP2B6*14* (R140Q), and *CYP2B6*15* (I391N) were genotyped by PCR–restriction fragment length polymorphism (PCR–RFLP) or allele-specific PCR (AS-PCR) methods. PCR was performed in a final volume of 25 μl, consisting of genomic DNA (100 ng), 1 × PCR buffer [67(mmol/l Tris–HCl buffer (pH 8.8), 16.6 mmol/l $(NH_4)_2SO_4$, 0.45% Triton X-100, 0.02% gelatin], 1.0–3.0 mmol/l $MgCl_2$, 0.4 μmol/l of each primer, 250 μmol/l dNTPs, and 1 U of *Taq* DNA polymerase. After an initial denaturation at 94°C for 3 min, the amplification was performed by denaturation at 94°C for 30 s, annealing for 30 s, and extension at 72°C for 30–90 s for 30 cycles. The final extension step was performed at 72°C for 5 min. The sequence of primers used in this study is summarized in Table 1. Primer sets, restriction enzymes for PCR–RFLP analyses, annealing temperatures, and fragment lengths are summarized in Table 2.

If participants were genotyped as heterozygotes for both c.516G > T (Q172H) and c.785A > G (K262R), they would be either *CYP2B6*1/CYP2B6*6* or *CYP2B6*4/ CYP2B6*9*. To determine the diplotype, we established a genotyping method. In the first step PCR, the *CYP2B6* gene was specifically amplified with the *CYP2B6*-specific PCR primers of 2B6*6-S and 2B6*6-AS (Table 1) to separate it from the *CYP2B7* gene. Genomic DNA samples (100 ng) were added to a PCR mixture (25 μl) consisting of 1 × PCR buffer (Takara), 0.25 mmol/l dNTPs, 0.4 μmol/l each primer, 1 U of Ex Taq polymerase. After an initial denaturation at 94°C for 3 min, the

Table 1 Oligonucleotides used for genotyping of *CYP2B6, CYP3A5*, and *ALDH1A1* alleles

Gene	Location	Primer	Sequence 5'–3'
CYP2B6	5'-UTR	2B6*1H-S	ACT TTC TGG TTT TAC GGC TCA
		2B6 T-2320C-S	AAT TTC TCT CTT TTG TGC TCT G
		2B6 T-2320C-AS	TGT GTC TCT GTT TTC CCC CT
		2B6 T-750C-S	GGA TGT GTG GGT GAA GGT G
		2B6 T-750C-AS	TTT TAT ATA CGA AAG TGC ATT TAC
		2B6 T-750C-W-AS	TCT GTA CTA AAA ACA CAA AAA TTA A
		2B6 T-750C-M-AS	TCT GTA CTA AAA ACA CAA AAA TTA G
		2B6*11-S	GCT CCT GGA TGA TGA TGA AAA
	Intron 1	2B6*11-AS	TAC TCA CCA ACC ATG CCC G
		2B6*12-S	TTT CCC GTC GGA CCC CT
	Exon 2	2B6*12-W-AS	GTC GAC CAT GGC GAT TTT TC
		2B6*12-M-AS	GTC GAC CAT GGC GAT TTT TT
	Exon 3	2B6*8-S	TGA TCT TTG CCA ATG GAA ACC
		2B6*14-W-S	ACT TCG GGA TGG GAA AGC G
		2B6*14-M-S	ACT TCG GGA TGG GAA AGC A
	Intron 3	2B6*8-AS	GTC TCC AGT TTC GTC TGT CT
		2B6 int3-S	GCT GTT ACG GTT ATT CTC ATG
		2B6*6-S	GTC AAA TTA CTC AGC CTC TCG
		2B6*9-S	CTT GAC CTG CTG CTT CTT CC
	Exon 4	2B6 Q172H-W-S	CCC CAC CTT CCT CTT CCA G
		2B6 Q172H-M-S	CCC CAC CTT CCT CTT CCA T
	Intron 4	2B6*9-AS	TCC CTC TCC GTC TCC CTG
		2B6 int3-AS	TGT CTG CGT TTC TTC CAA GG
		2B6*4-S	GGC GCT CTC TCC CTG TGA
	Intron 6	2B6*4-AS	CCT ACA GTG CTC CCA GAA TA
		2B6*6-AS	AGA GCC TAC AGT GCT CCC A
	Intron 7	2B6*15-S	GGC ATC CTG GAT TCT CTT AAT
	Intron 8	2B6*15-AS	GGA TAA GGC AGG TGA AGC AA
		2B6*5-S	TGA GAA TCA GTG GAA GCC ATA GA
	Exon 9	2B6*5-AS	TAA TTT TCG ATA ATC TCA CTC CTG C
CYP3A5	Intron 3	3A5*3-S	CTT TAA AGA GCT CTT TTG TCT CTC A
		3A5*3-AS	CCA GGA AGC CAG ACT TTG AT
	Intron 4	3A5*5-S	ACA TAC ACT CAG AAG AGG CTA GGC
	Intron 5	3A5*5-AS	TAG GAA GCT CGA ACT CAG TGG ACT
	Intron 6	3A5*4-S	CGC CAC CTT TCT TGA ATC CAC T
	Intron 7	3A5*4-AS	GGA ATT GTA CCT TTT AAG TGG ATG
	Intron 10	3A5*7-W-S	TTC CTT CCA GGC ACC ACC TA
		3A5*7-M-S	TTC CTT CCA GGC ACC ACC TT
	Exon 11	3A5*2-S	ACC ACC TAC CTA TGA TGC CG
	Intron 11	3A5*2-AS	TTG ATT ATC TTT GTC TTG TGC TG
ALDH1A1	5'-UTR	ALDH1A1*3-W-S	CTA ACT TAG GGT AGG GTG TAG A
		ALDH1A1*3-M-S	CTA ACT TAG GGT AGG GTG TAG T
		ALDH1A1*3-AS	ATT TTT TTG ACT TCT CAT GCT TTT TA

amplification was performed by denaturation at 94°C for 30 s, annealing at 57°C for 30 s, and extension at 72°C for 4 min for 30 cycles. Next, AS-PCR was performed. The diluted product of the first PCR was added to a PCR mixture (25 μl) consisting of 1 × PCR buffer (Takara), 0.25 mmol/l dNTPs, 0.4 μmol/l of 2B6*4-AS primer, 0.4 μmol/l of 2B6-Q172H-W-S or 2B6-Q172H-M-S primer (Table 1), and 1 U of Ex Taq polymerase. After an initial denaturation at 94°C for 3 min, the amplification was performed by denaturation at 94°C for 30 s, annealing at 63°C for 30 s, and extension at 72°C for 4 min for 15 cycles. To detect the SNP c.785A > G, the PCR product was digested with *Sty* I restriction enzymes. The digestion patterns were determined by electrophoresis in a 2% agarose gel. If the diplotype is *CYP2B6*1/CYP2B6*6*, the PCR product with 2B6-Q172H-W-S shows 903, 886, 576, 498, 251, 171, and 56 bp fragments and the PCR product with 2B6-Q172H-M-S shows 1074, 886, 576, 498, 251, and 56 bp fragments. If the diplotype is *CYP2B6*4/CYP2B6*9*, the PCR product with 2B6-

Q172H-W-S shows 1074, 886, 576, 498, 251, and 56 bp fragments, and the PCR product with 2B6-Q172H-M-S shows 903, 886, 576, 498, 251, 171, and 56 bp fragments.

Direct sequence analyses of exons and exon–intron junctions, and the 5'-flanking region (up to –3.3 kb) were performed to examine the nucleotide sequences of the *CYP2B6* gene in a homozygote of the *CYP2B6*1* allele with the lowest AUC ratio of 4-OH-CPA/CPA. A Thermo Sequenase Cy5.5 Dye Terminator Cycle Sequencing kit (Amersham Pharmacia Biotech, Buckinghamshire, UK) was used with a Long-Read Tower DNA sequencer (Amersham Pharmacia Biotech).

The SNPs g.–2320T > C, g.–750T > C, g.15582C > T (intron 3), and g.18492T > C (intron 5) were genotyped by PCR–RFLP or AS-PCR methods. The primer sets, annealing temperatures, restriction enzymes, and fragment lengths are summarized in Table 2. The alleles possessing g.–2320T > C and g.–750T > C are

Table 2 Genotyping method by PCR–RFLP or AS-PCR

Polymorphism Genomes	cDNA (amino acid change)	Primer set	PCR–RFLP or AS-PCR	Concentration of MgCl₂(mmol/l)	Temperature for annealing (°C)	Fragment length (bp)	Electrophoresis
CYP2B6							
g.−2320T>C		2B6 T-2320C-S 2B6 T-2320C-AS	RFLP (EcoR V)	1.5	57	wt: 940, 105 mt: 1045	0.8% agarose
g.−750T>C		2B6 T-750C-S 2B6 T-750C-AS	RFLP (Mse I)	1.5	57	wt: 732, 210, 26 mt: 732, 236	4% agarose
g.136A>G	c.136A>G (M46V)	2B6*11-S 2B6*11-AS	RFLP (EcoN I)	1.5	57	wt: 293, 131 mt: 258, 131, 35	2% agarose
g.12820G>A	c.296G>A (G99E)	2B6*12-S 2B6*12-W-AS or 2B6*12-M-AS	AS-PCR	1	57	274	2% agarose
g.13072A>G	c.415A>G (K139E)	2B6*8-S 2B6*8-AS	RFLP (BsrB I)	1.5	57	wt: 173, 95 mt: 173, 80, 15 205	2% agarose
g.13076G>A	c.419G>A (R140Q)	2B6*14-W-S or 2B6*14-M-S 2B6*8-AS	AS-PCR	1	57		2% agarose
g.15582C>T		2B6 int3-S 2B6 int3-AS	RFLP (BfuA I)	1	57	wt: 292, 116 mt: 408	2% agarose
g.15631G>T	c.516G>T (Q172H)	2B6*9-S 2B6*9-AS	RFLP (Bsr I)	1.5	60	wt: 204 mt: 152, 52	4% agarose
g.18053A>G	c.785A>G (K262R)	2B6*4-S 2B6*4-AS	RFLP (Sty I)	1.5	57	wt: 903, 171, 33 mt: 1074, 33	0.8% agarose
g.18492T>C		2B6*4-S 2B6*4-AS	RFLP (Hinf I)	1.5	57	wt: 1107 mt: 642, 465	0.8% agarose
g.21388T>A	c.1172T>A (I391N)	2B6*15-S 2B6*15-AS	RFLP (Fok I)	1.5	57	wt: 168, 156, 99 mt: 255, 168	4% agarose
g.25505C>T	c.1459C>T (R487C)	2B6*5-S 2B6*5-AS	RFLP (Bgl II)	1.5	60	wt: 1400 mt: 1186, 214	0.8% agarose
CYP3A5							
g.6986A>G		3A5*3-S 3A5*3-AS	RFLP (Dde I)	1.5	56	wt: 129, 71 mt: 107, 71, 22	3% agarose
g.12952T>C		3A5*5-S 3A5*5-AS	RFLP (Hsp92 II)	1.5	56	wt: 276, 134 mt: 167, 134, 109	3% agarose
g.14665A>G	c.598A>G (Q200R)	3A5*4-S 3A5*4-AS	RFLP (BsmA I)	1.5	56	wt: 455, 130, 60 mt: 277, 178, 130, 60	2% agarose
g.27131 insT	c.1031 insT	3A5*7-W-AS or 3A5*7-M-AS 3A5*2-AS	AS-PCR	1.5	58	455	2% agarose
g.27289C>A	c.1189C>A (T398N)	3A5*2-S 3A5*2-AS	RFLP (Tsp509 I)	1.5	56	wt: 360, 83 mt: 197, 163, 83	2% agarose
ALDH1A1							
g.−523 insATG		ALDH1A1*3-W-S or ALDH1A1*3-M-S ALDH1A1*3-AS	AS-PCR	2	61	249	2% agarose

mt, mutant type; wt, wild type.

CYP2B6*1B and CYP2B6*1G, respectively [10]. The allele possessing both g.−2320T > C and g.−750T > C is the CYP2B6*1H allele. If participants were genotyped as heterozygotes for both g.−2320T > C and g. −750T > C, they would be either CYP2B6*1A/CYP2B6*1H or CYP2B6*1B/CYP2B6*1G. To determine the diplotype, we established a genotyping method. Genomic DNA samples (100 ng) were added to a PCR mixture (25 μl) consisting of 1 × PCR buffer (Takara), 0.25 mmol/l dNTPs, 0.4 μmol/l of 2B6*1H-S primer, 0.4 μmol/l of 2B6 T-750C-W-AS or 2B6 T-750C-M-AS primer (Table 1), and 1 U of Taq DNA polymerase. After an initial denaturation at 94°C for 3 min, the amplification was performed by denaturation at 94°C for 30 s, annealing at 61°C for 30 s, and extension at 72°C for 2 min for 30 cycles. To detect the SNP g.−2320T > C,

the PCR product was digested with EcoR V restriction enzymes. The digestion patterns were determined by electrophoresis in a 0.8% agarose gel. If the diplotype is CYP2B6*1A/CYP2B6*1H, the PCR product with 2B6 T-750C-W-AS shows 1696 and 182 bp fragments and the PCR product with 2B6 T-750C-M-AS shows a 1778 bp fragment. If the diplotype is CYP2B6*1B/CYP2B6*1G, the PCR product with 2B6 T-750C-W-AS shows a 1778 bp fragment and the PCR product with 2B6 T-750C-M-AS shows 1696 and 182 bp fragments.

Linkage disequilibrium (LD) analysis for the SNPs of the CYP2B6 gene was performed using SNPAlyze software (Dynacom, Yokohama, Japan), and pairwise two-dimensional maps between SNPs were obtained for the |D'| values.

Genotyping of CYP2C19, CYP3A4, and CYP3A5 alleles

CYP2C19*2 (splicing defect) and CYP2C19*3 (W212X) were genotyped as described previously [24]. CYP3A4*4 (I118V), CYP3A4*5 (P218R), CYP3A4*6 (frameshift), CYP3A4*16 (T185S), and CYP3A4*17 (F189S) alleles were genotyped as we previously reported [25]. CYP3A5*2 (T398N), CYP3A5*3 (splicing defect), CYP3A5*4 (Q200R), CYP3A5*5 (splicing defect), and CYP3A5*7 (frameshift) were genotyped by PCR–RFLP or AS-PCR methods. The primer sets, annealing temperatures, restriction enzymes, and fragment length are summarized in Table 2.

Genotyping of ALDH1A1 and GST alleles

ALDH1A1*3 (−523 insATG) was genotyped by the AS-PCR method. The primer sets, annealing temperatures, and fragment length are also summarized in Table 2. GSTA1*B (g.−631T > G, g.−567T > G, g.−69C > T, g.−52G > A) and GSTP1*B (I105V) alleles were genotyped as described previously [26,27]. Null alleles of GSTM1 and GSTT1 were genotyped by the multiplex PCR method reported by Chen et al. [28] with a slight modification of the antisense primer for GSTT1 (5′-GCCTTCAGAATGACCTCATG-3′). β-Globin was coamplified and used as an internal control. The amplified product was visualized in an ethidium bromide-stained 2% agarose gel. The expected sizes of GSTM1, GSTT1, and β-globin were 215, 388, and 268 bp, respectively. When no PCR product was detected despite the presence of β-globin, it was considered to be a null genotype.

Analysis of adverse reactions

Adverse reactions in each patient were assessed in the course of chemotherapy in which pharmacokinetics were analyzed. As indicators of myelosuppression, leukocytes and neutrophils were counted after drug administration. The nadirs of the counts were used as reflecting the maximal myelosuppression. The other adverse reactions analyzed were gastrointestinal toxicity and alopecia. These toxicities were assessed on the basis of common toxicity criteria grading (NCI-CTC version 2). The highest grades observed throughout all courses were assessed. Although the data of myelosuppression were obtained from all patients, the data of gastrointestinal toxicity and alopecia were obtained from 89 patients.

Statistical analyses

Fisher's exact test was used to verify agreement of the observed genotype frequencies with the expected ones (Hardy–Weinberg equilibrium). Pharmacokinetic data are presented as mean ± SD. Data were evaluated for equal variance by the Bartlett F-test using an SPSS computer package (Version 13.0, SPSS, Chicago, Illinois, USA). Mann–Whitney U-test was used to investigate the sex and group differences in the pharmacokinetic parameters. The relationship between the pharmacokinetic para-

meters and CTC grades, and the relationship between the percentage decrease in leukocyte or neutrophil count and CYP2B6 genotypes were investigated by Kruskal–Wallis test and Steel–Dwass test. The relationships between the pharmacokinetic parameters and genotypes were investigated by one-way analysis of variance and Tukey's test. The statistical significance of differences in the incidence of severe toxicity between the CYP2B6 genotypes was tested by Fisher's exact method. $P < 0.05$ was considered statistically significant.

Results

Pharmacokinetic parameters of cyclophosphamide and 4-hydroxycyclophosphamide

The pharmacokinetic parameters of CPA and 4-OH-CPA are shown in Table 3. Dose of CPA for patients with malignant lymphoma was significantly higher than that for patients with breast cancer. The AUC and $t_{1/2}$ of CPA as well as the AUC of 4-OH-CPA in patients with malignant lymphoma were significantly higher than those in patients with breast cancer. No statistical difference in the AUC ratio of 4-OH-CPA/CPA was, however, calculated as the metabolic index between the two population groups. In patients with malignant lymphoma, women showed significantly higher AUC values of CPA and 4-OH-CPA than men. No sex difference was observed in the AUC ratio of 4-OH-CPA/CPA. Therefore, the CL of CPA and the AUC ratio of 4-OH-CPA/CPA in all patients were collectively analyzed in the subsequent analyses. In overall patients ($n = 103$), the interindividual difference in the CL of CPA was approximately 15-fold (1.4–20.5 l/h). The interindividual variability of the AUC ratio of 4-OH-CPA/CPA was as high as 54-fold (0.001–0.054).

Adverse reactions

Leukocytopenia of grades 3 and 4 was observed in 40 and 16 patients, respectively. Neutropenia of grades 3 grade 4 was observed in 24 and 35 patients, respectively. Gastrointestinal toxicity of grade 3, as evidenced by severe nausea and vomiting, was observed in five patients, and severe alopecia of grade 2 was observed in 20 patients. Figure 2 shows scatterplots of the toxicity grade versus the AUC of 4-OH-CPA. The patients suffering from severe leukocytopenia or neutropenia had significantly ($P < 0.05$) higher AUC of 4-OH-CPA, supporting the previous finding that 4-OH-CPA is an active metabolite. As the AUC of 4-OH-CPA in patients with malignant lymphoma was significantly higher than that in patients with breast cancer, patients with malignant lymphoma seemed to have severer myelosuppression than patients with breast cancer.

Genetic polymorphisms of CYPs genes

The allele frequencies of the CYP2B6*4, CYP2B6*5, CYP2B6*6, and CYP2B6*9 in the 103 Japanese cancer patients were 5.3, 0.5, 18.4, and 1.0, respectively (Table 4). The genotype frequencies were in the Hardy–Weinberg

Table 3 Pharmacokinetic parameters of CPA and 4-OH-CPA (n=103)

| | Malignant lymphoma (Regimen: CHOP or R-CHOP) | | | Breast cancer (Regimen: AC) | | |
	Men (n=26)	Women (n=26)	Total (n=52)	Women (n=51)	Total (n=103)	Range
Dose (mg/body) CPA	1196±191	1065±127††	1131±174**	870±110	1002±195	(600–1500)
AUC (μmol/l·h)	1125.8±412.8	1139.3±468.4††	1132.6±437.2**	774.8±241.9	955.4±395.7	(256.8–2261.8)
CL (l/h)	4.5±3.5	3.9±2.2	4.2±2.9	4.0±1.3	4.1±2.3	(1.4–20.5)
$t_{1/2}$ (h)	7.0±2.3	6.3±1.9	6.6±2.1*	5.7±1.6	6.2±1.9	(2.6–11.7)
4-OH-CPA AUC (μmol/l·h)	13.7±6.5	17.3±11.3††	15.5±9.3**	9.4±5.7	12.5±8.3	(0.7–56.6)
AUC ratio 4-OH-CPA/CPA	0.015±0.012	0.018±0.013	0.017±0.013	0.014±0.011	0.015±0.012	(0.001–0.054)

Data are mean±SD.
*P<0.05, **P<0.005, compared with patients with breast cancer (women, n=51) by Mann–Whitney U-test.
††P<0.005, compared with men patients with malignant lymphoma (n=26) by Mann–Whitney U-test.

Fig. 2
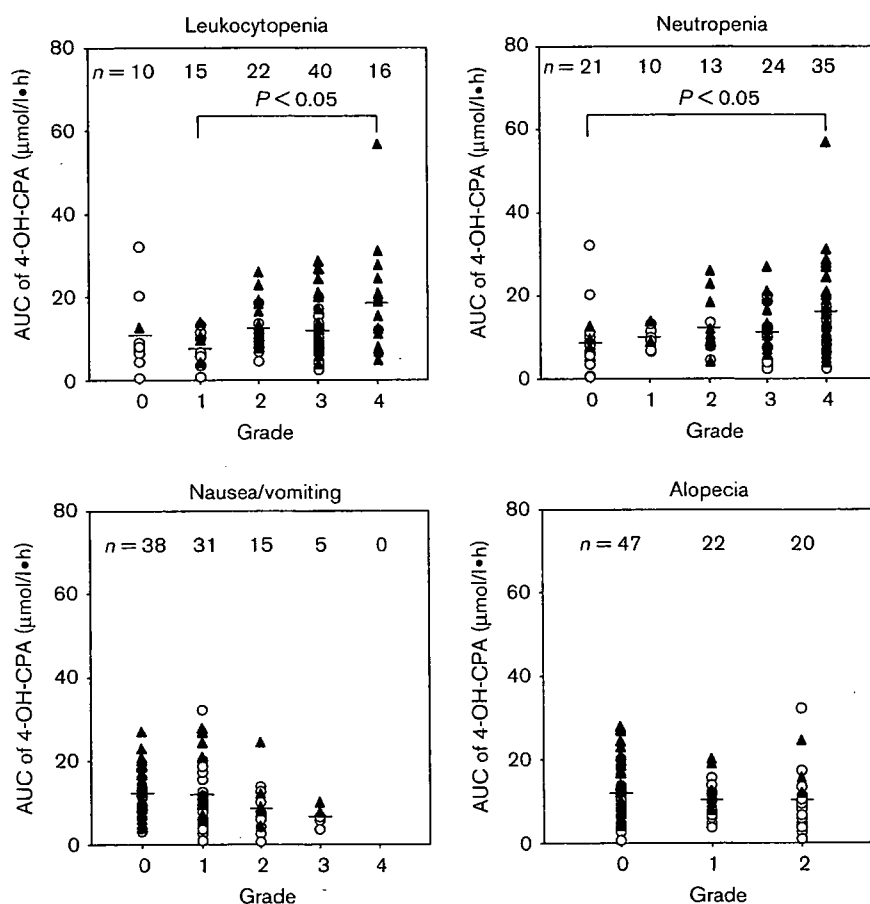
Scatterplots depicting the toxicity grades based on common toxicity criteria grading versus the area under the curve (AUC) of 4-hydroxycyclophosphamide (4-OH-CPA). Closed triangle and open circle represent the patients with malignant lymphoma and breast cancer, respectively. Statistical significance (P<0.01) was observed between leukocytopenia or neutropenia and the AUC of 4-OH-CPA by Kruskal–Wallis test and Steel–Dwass test.

equilibrium (P values were higher than 0.141). No patient had the CYP2B6*8, CYP2B6*11, CYP2B6*12, CYP2B6*14, or CYP2B6*15 alleles. These results were in accordance with previous studies in Japanese [13,29]. A patient having the lowest metabolic potency (AUC ratio of 4-OH-CPA/CPA was 0.001) was genotyped as a homozygote of the CYP2B6*1 allele. To investigate whether unknown novel mutation(s) might exist in the CYP2B6 gene, we performed direct sequence analyses. Consequently, we found that this patient was hetero-

Table 4 Allele frequencies of *CYPs*, *ALDH*, and *GST* genes in Japanese cancer patients (*n*=103)

Allele	Effect	Allele frequency (%)
CYP2B6*4	K262R	5.3
CYP2B6*5	R487C	0.5
CYP2B6*6	Q172H, K262R	18.4
CYP2B6*7	Q172H, K262R, R487C	0
CYP2B6*8	K139E	0
CYP2B6*9	Q172H	1.0
CYP2B6*11	M46V	0
CYP2B6*12	G99E	0
CYP2B6*14	R140Q	0
CYP2B6*15	I391N	0
CYP2C19*2	Splicing defect	31.1
CYP2C19*3	W212X	12.6
CYP3A4*4	I118V	0
CYP3A4*5	P218R	0.5
CYP3A4*6	Frameshift	0
CYP3A4*16	T185S	2.4
CYP3A4*17	F189S	0
CYP3A5*2	T398N	0
CYP3A5*3	Splicing defect	75.7
CYP3A5*4	Q200R	0
CYP3A5*5	Splicing defect	0
CYP3A5*7	Frameshift	0
ALDH1A1*3	g. - 523 insATG	0
GSTA1*B	g. - 631T>G, g. - 567T>G, g. - 69C>T, g. - 52G>A	13.6
GSTM1*O	Null	54.4[a]
GSTP1*B	I105V	15.0
GSTT1*O	Null	49.5[a]

[a]Null genotype frequency, not allele frequency.

zygous for four SNPs, g.-2320T > C, g.-750T > C, g.15582C > T (intron 3), and g.18492T > C (intron 5). Although three SNPs, g.-2320T > C, g.-750T > C, and g.15582C > T, had been already reported [10], the SNP g.18492T > C was first found in this study. Next, all patients were subjected to the genotyping of these SNPs in the 5'-flanking region and introns, regardless of the presence or absence of SNPs in coding region. The frequencies of the SNPs g.-2320T > C and g.-750T > C were 51.9 and 68.4%, respectively. The allele frequencies of *CYP2B6*1B* (g.-2320T > C), *CYP2B6*1G* (g.-750T > C), and *CYP2B6*1H* (g.-2320T > C and g.-750T > C) were 1.0, 17.5, and 51.0%, respectively. The frequencies of the SNPs g.15582C > T, and g.18492T > C were 81.6 and 70.9%, respectively. The extent of LD within the *CYP2B6* gene is shown in Fig. 3. A strong LD was shown between the SNPs c.516G > T (Q172H) and c.785A > G (K262R). In addition, high LD was shown between the SNPs in the 5'-flanking region and introns.

The allele frequencies of *CYP2C19*2* and *CYP2C19*3* were 31.1 and 12.6%, respectively (Table 4), and these were consistent with previous results from healthy Japanese participants [30]. The *CYP3A4*5* and *CYP3A4*16* alleles were found with frequencies of 0.5 and 2.4%, respectively, but the *CYP3A4*4*, *CYP3A4*6*, and *CYP3A4*17* alleles were not found in this study. Among 103 patients, 38 and 59 patients were heterozygotes and

Fig. 3
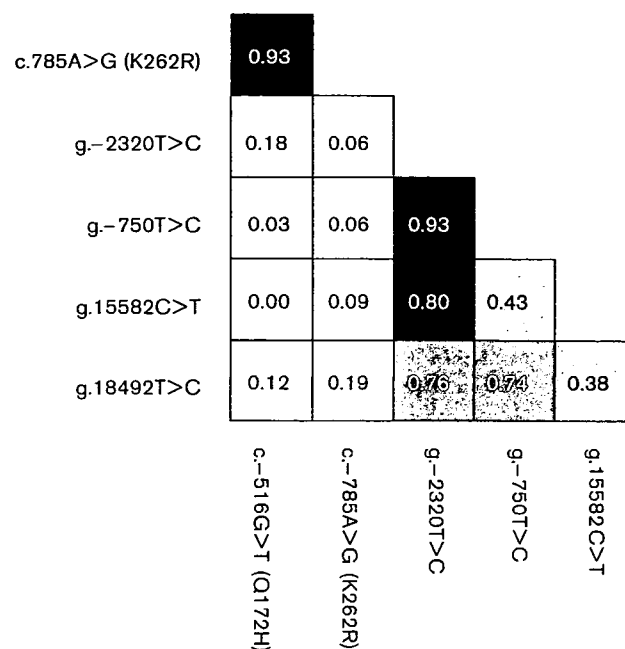
Linkage disequilibrium (LD) analysis of *CYP2B6* single nucleotide polymorphisms (SNPs). A standard shading scheme is used to display LD, with dark shade indicating very strong LD (|D'|=0.8–1), white indicating no LD (|D'|<0.2), and light shades indicating intermediate LD. The SNP leading the amino acid change R487C in the *CYP2B6*5* allele was not included in this analysis, because this allele was found in only a patient heterozygously.

homozygotes of *CYP3A5*3*, respectively resulting in an allele frequency of 75.7%. No patient had the *CYP3A5*2*, *CYP3A5*4*, *CYP3A5*5*, *CYP3A5*7* alleles. These frequencies of the *CYP3A* alleles were comparable to those of previous reports in Japanese participants [29,31].

Genetic polymorphisms of *ALDH1A1* and *GST* genes

No patient had the *ALDH1A1*3* allele. The allele frequencies of *GSTA1*B* and *GSTP1*B* were 13.6 and 15.0%, respectively (Table 4). The *GSTM1*O* (*GSTM1* null) and *GSTT1*O* (*GSTT1* null) genotype were found in 56 and 51 patients, respectively. Among them, 33 patients had the double-null genotype. These frequencies were comparable to those of previous reports [26,32,33].

Effects of genetic polymorphisms of drug-metabolizing enzymes on pharmacokinetics of cyclophosphamide and 4-hydroxycyclophosphamide

The relationship between the CL of CPA or AUC ratios of 4-OH-CPA/CPA and the genotypes of drug metabolism enzymes were investigated. The CL of CPA in homozygotes of *CYP2B6*6* (9.2 ± 9.8 l/h) was significantly ($P < 0.05$) higher than that in homozygotes of *CYP2B6*1* (3.8 ± 1.5 l/h) or heterozygotes of *CYP2B6*1/*6* (3.8 ± 1.5 l/h) (Fig. 4a). The possibility could not be

Fig. 4
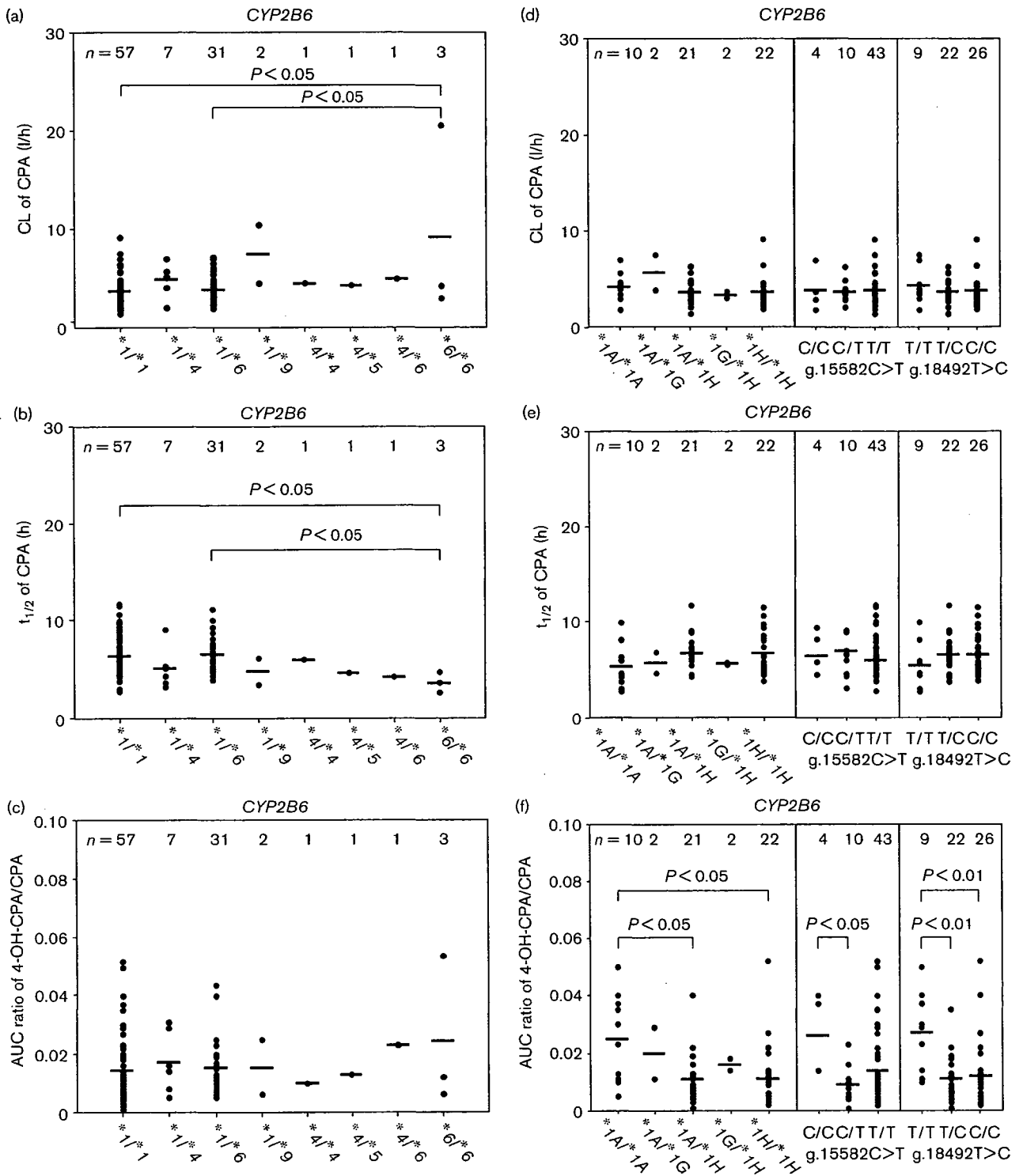
Pharmacokinetic parameters of cyclophosphamide (CPA) and 4-hydroxycyclophosphamide (4-OH-CPA) in cancer patients with different genotypes of the CYP2B6 gene. The clearance of CPA (a and d), half-life of CPA (b and e), and the area under the curve (AUC) ratio of 4-OH-CPA/CPA (c and f) were analyzed. Each point represents an individual, and the mean value in each genotype is shown with a bar. CL, clearance.
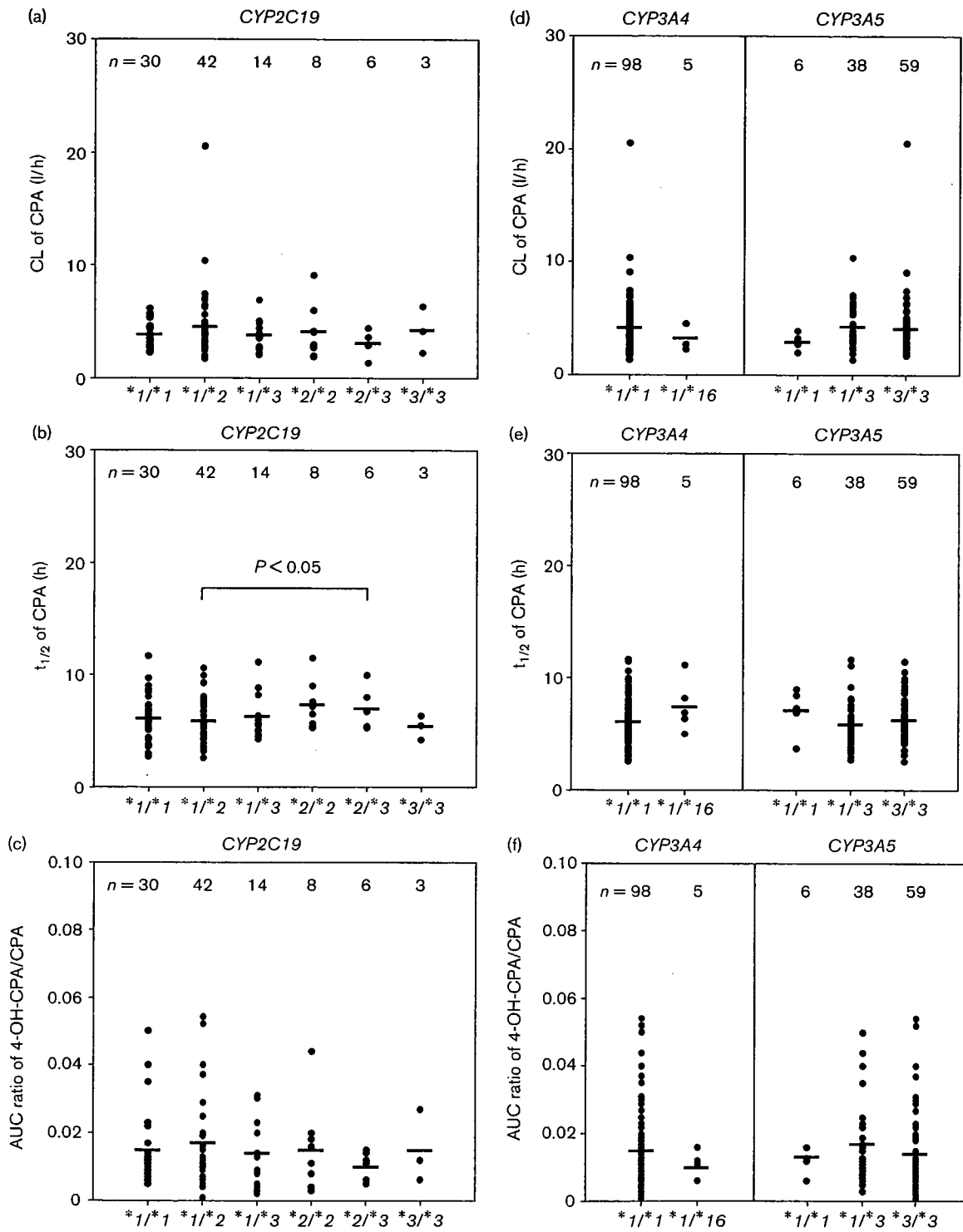
Fig. 5

Pharmacokinetic parameters of cyclophosphamide (CPA) and 4-hydroxycyclophosphamide (4-OH-CPA) in cancer patients with different genotypes for *CYP2C19* (a–c) and *CYP3A* (d–f) genes. The clearance of CPA (A and D), half-life of CPA (b and e), and the area under the curve (AUC) ratio of 4-OH-CPA/CPA (c and f) were analyzed. Each point represents an individual (*n* = 103), and the mean value in each genotype is shown with a bar.

denied, however, that the data from one outlier in homozygotes of *CYP2B6*6* affected the statistical analysis. The half-life of CPA in homozygotes of *CYP2B6*6* (3.6 ± 1.0 h) was significantly ($P < 0.05$) shorter than that in homozygotes of *CYP2B6*1* (6.3 ± 2.0 h) or heterozygotes of *CYP2B6*1/*6* (6.5 ± 1.7 h) (Fig. 4b). The AUC ratios were not different between different genotypes of the *CYP2B6* alleles leading to amino acid changes (Fig. 4c). Next, the SNPs in the 5'-flanking region or introns were analyzed for the relationship with the pharmacokinetic parameters. In this analysis, to exclude the effects of SNPs in coding region, the data from the homozygotes of *CYP2B6*1* ($n = 57$) were used. As shown in Fig. 4f, the participants with *CYP2B6*1A/*1H* (0.011 ± 0.009) or the participants with *CYP2B6*1H/*1H* (0.011 ± 0.011) showed significantly ($P < 0.05$) lower AUC ratios than the participants with *CYP2B6*1A/*1A* (0.025 ± 0.015). Heterozygotes of g.15582 T (0.009 ± 0.006) showed significantly ($P < 0.05$) lower AUC ratios than homozygotes of g.15582C (0.026 ± 0.014). In addition, heterozygotes (0.011 ± 0.008) and homozygotes (0.012 ± 0.012) of g.18492C showed significantly ($P < 0.01$) lower AUC ratios than homozygotes of g.18492 T (0.027 ± 0.014).

As shown in Fig. 3, the SNPs in 5'-flanking region or introns showed low LD with the SNPs c.516G > T and c.785A > G. The SNPs in the 5'-flanking region or introns were, however, actually found in the participants possessing the SNPs in the coding region. We investigated the relationship between the pharmacokinetic and the SNPs in the 5'-flanking region in 46 participants possessing the SNPs in the coding region. Among the participants genotyped as *CYP2B6*1/*4* or *CYP2B6*1/*6*, classification based on the SNPs in the 5'-flanking region did not find any relationship with the pharmacokinetics (data not shown). The other participants genotyped as *CYP2B6*1/ *9*, *CYP2B6*4/*4*, *CYP2B6*4/*5*, *CYP2B6*4/*6*, and *CYP2B6*6/*6* could not be investigated for the effects of the SNPs in the 5'-flanking region, because of the small sample size. Thus, definitive conclusion could not be drawn by the combination analysis for the SNPs in noncoding and coding region.

Concerning the genetic polymorphisms of *CYP2C19*, no relationship was observed between the CL of CPA and AUC ratio of 4-OH-CPA/CPA (Fig. 5a and c). Although there was no statistical difference in the half-life of CPA in homozygotes of *CYP2C19*1* (6.1 ± 2.1 h) and heterozygotes of *CYP2C19*1/*2* (5.9 ± 1.9 h), the half-life in heterozygotes of *CYP2C19*2/*3* (7.0 ± 1.8 h) was significantly ($P < 0.05$) longer than in heterozygotes of *CYP2C19*1/*2* (Fig. 5b). In addition, homozygotes of *CYP2C19*2* (7.3 ± 2.1 h) tend to show longer half-lives. Concerning the genetic polymorphisms of *CYP3A4* and *CYP3A5*, no relationship was observed between the CL

Table 5 Association of *CYP2B6* genotypes and leukocytopenia in Japanese cancer patients (*n*=57)

	Leukocytopenia (grade ≥ 2)		The percent decrease in leukocyto count [(baseline–nadir)/ baseline] × 100 (%)
	Not experienced	Experienced	
CYP2B6*1A/*1A (*n*=10)	0 (0%)	10 (100%)*	72.3 ± 18.1
CYP2B6*1A/*1H (*n*=21)	4 (19%)	17 (81%)*	59.1 ± 21.5
CYP2B6*1H/*1H (*n*=22)	9 (41%)	13 (59%)*	51.2 ± 32.9
CYP2B6*1A/*1G (*n*=2)	0 (0%)	2 (100%)	(43.6, 58.2)
CYP2B6*1G/*1H (*n*=2)	0 (0%)	2 (100%)	(55.0, 90.4)
g.15582C>T			
C/C (*n*=4)	0 (0%)	4 (100%)	79.3 ± 16.3
C/T (*n*=10)	2 (20%)	8 (80%)	63.5 ± 24.4
T/T (*n*=43)	11 (26%)	32 (74%)	55.5 ± 27.0
g.18492T>C			
T/T (*n*=9)	0 (0%)	9 (100%)*	75.6 ± 16.0[†]
T/C (*n*=22)	3 (14%)	19 (86%)*	60.9 ± 20.9
C/C (*n*=26)	10 (38%)	16 (62%)*	50.7 ± 30.8[†]

*$P < 0.05$, by Fisher's exact method.
[†]$P < 0.05$, by Kruskal–Wallis and Steel–Dwass test.
Data from the subjects genotyped as *CYP2B6*1A/*1G* and *CYP2B6*1G/*1H* were not included in the statistical analysis.

and half-life of CPA, and the AUC ratio of 4-OH-CPA/ CPA (Fig. 5d–f). No relationship between the AUC of 4-OH-CPA and the genotypes of *GSTs* was observed (data not shown).

Association between *CYP2B6* genotypes and adverse reaction of cyclophosphamide

Of the drug-metabolizing enzymes examined in this study, only the genotypes of the *CYP2B6* gene were associated with adverse reactions from CPA (Table 5). All of 10 patients with *CYP2B6*1A/*1A* (100%) developed severe (≥ grade 2) leukocytopenia. In contrast, the percentages of the patients developing severe leukocytopenia were decreased with *CYP2B6*1H* allele (81% in *CYP2B6*1A/*1H* and 59% in *CYP2B6*1H/*1H*) ($P < 0.05$). Similarly, all of nine homozygotes of g.18492 T (100%) developed severe leukocytopenia, compared with 86% of the heterozygotes or 62% of the homozygotes of g.18492C ($P < 0.05$). These results suggested that the SNPs were associated with the decreased risk of leukocytopenia. The percentage decrease in leukocyte count [(baseline-nadir)/baseline] was larger in the patients with *CYP2B6*1A/*1A* (72.3 ± 18.1%) than in patients with *CYP2B6*1A/*1H* (59.1 ± 21.5%) or *CYP2B6*1H/*1H* (51.2 ± 32.9%), although there was no statistical difference (Table 5). It was significantly larger in the homozygotes of g.18492 T (75.6 ± 16.0%) than in homozygotes of g.18492C (50.7 ± 30.8%). Similar tendency was observed in the percentage decrease in neutrophil count although these were statistically insignificant (data not shown). Thus, the patients possessing the SNPs g. –2320T > C, g.

−750T > C, and g.18492T > C showed less adverse reaction. The results suggested that these SNPs would be a good predictor of toxicity.

Discussion

The treatment of cancer with drugs requires a dose high enough to achieve the maximal antitumor effects, but low enough to avoid serious side effects, resulting in a narrow therapeutic range. Anticancer drugs have wide interindividual variation in the responses owing to the pharmacokinetic variability. One of the causes of the variation in drug effects is genetic polymorphisms of drug-metabolizing enzymes. Much progress has been made over the last decade in understanding the relationship between genetic polymorphisms of drug-metabolizing enzymes and interindividual variability in the drug response. For cancer therapy, the correlation has also been the subject of much research concerning, for example, thiopurine methyltransferase for 6-mercaptopurine [34], dihydropyrimidine dehydrogenase for 5-fluorouracil [35], and UDP-glucuronosyltransferase for irinotecan [36]. In this study, we focused on CPA. CPA is a prodrug, which exerts its effect after hepatic bioactivation to 4-OH-CPA by CYP2B6. In addition, CYP2C19, CYP3A4, and CYP3A5 are also involved in this metabolic activation pathway [2,3,4,21]. Alternatively, 4-OH-CPA was found to be inactivated through ALDH1A1 and GSTs [7,8]. We sought to study the interindividual variability in the pharmacokinetics of CPA and 4-OH-CPA and its association with genetic polymorphisms of drug-metabolizing enzymes in Japanese cancer patients.

In contrast to the previous study by Xie *et al.* [18] reporting that Caucasian Q172H carriers showed higher AUC ratios of 4-OH-CPA/CPA (0.027 ± 0.020) than noncarriers (0.017 ± 0.014), we found no association between the CPA 4-hydroxylation and the *CYP2B6*6* and *CYP2B6*9* alleles in Japanese patients. The discrepancy might be because of some factors including ethnic differences, the number of participants (eight carriers and 21 noncarriers in 29 Caucasians versus 37 carriers and 66 noncarriers in 103 Japanese), dose of CPA, or comedications. The current results regarding *CYP2B6*6* were in accordance with those in the study by Kirchheiner *et al.* [15], who reported that the in-vivo CL of bupropion did not differ between *CYP2B6*6* carriers and noncarriers. Kirchheiner *et al.* [15] also reported that the CL of bupropion in *CYP2B6*4* carriers was higher than that in wild participants. In addition, an in-vitro study with a heterologous expression system revealed that CYP2B6.4 showed higher activity compared with CYP2B6.1 (wild-type) [16]. In this study, although the heterozygotes of *CYP2B6*4* (0.017 ± 0.010) tended to show higher AUC ratios than homozygotes of *CYP2B6*1* (0.014 ± 0.012), the difference was statistically insignificant.

In Caucasians, the frequencies of g.−2320T > C and g.−750T > C have been reported to be 30.0 and 56.6%, respectively [37]. We first determined the frequencies of g.−2320T > C and g.−750T > C (51.9 and 68.4%, respectively) in Japanese participants. Zukunft *et al.* [37], using a luciferase assay, reported that g.−750T > C did not affect the transcriptional activity of the *CYP2B6* gene. There has been no report concerning the effects of g.−2320T > C on the transcriptional activity. As shown in Fig. 4f, we found that these SNPs, however, were significantly associated with decreased CPA 4-hydroxylation. We also found that the SNP g.15582C > T in intron 3 was associated with decreased CPA 4-hydroxylation. Lamba *et al.* [10] reported that this SNP was associated with a splicing variant lacking exons 4 to 6. In accordance with their report [10], a high degree of linkage was observed between the SNPs g.−2320T > C, g.−750T > C, and g.15582C > T. It remains to be clarified whether the effects of the SNP g.15582C > T on CYP2B6 activity might be associated with the splicing variant or be due to the linkage with SNP in the 5'-flanking region. In this study, we identified a novel SNP, g.18492T > C, in intron 5, which is common in Japanese participants (70.9%). This SNP was also associated with decreased CPA 4-hydroxylation. To investigate the possibility that the SNP might be associated with a splicing variant, we performed RT-PCR analyses using total RNA samples from 19 human livers. We could not find any product indicating a splicing variant (data not shown).

The *CYP2C19*2* and *CYP2C19*3* alleles were associated with defective enzyme function [38]. Timm *et al.* [19] demonstrated that *CYP2C19*2* carriers had lower elimination constants of CPA than noncarriers. Our study may possibly support this finding because the heterozygotes of *CYP2C19*2/*3* showed a significantly longer half-life of CPA than heterozygotes of *CYP2C19*1/*2*. Roy *et al.* [3] has reported that CYP2C19 could not practically contribute to CPA 4-hydroxylation in human livers (< 6% of the total activity). Therefore, the effects of the *CYP2C19* polymorphism on CPA metabolism could not be explained. Although the involvement of CYP2C9 in CPA metabolism has been demonstrated, its contribution is controversial [3,39,40]. In addition, the *CYP2C9* polymorphic alleles are very rare in Japanese [41]. Accordingly, we did not investigate the *CYP2C9* polymorphisms. The *CYP3A4*16* allele has been reported to be associated with decreased testosterone hydroxylase activity in a heterologous expression system [42]. In our study, no effects of the *CYP3A4*16* allele on CPA 4-hydroxylation were observed. This might be because of the small number of *CYP3A4*16* carriers ($n = 5$) or the minor contribution (12–18%) of CYP3A4 in CPA 4-hydroxylation in human liver microsomes [3]. CYP3A4 also has a role in N-dechloroethylation of CPA (10% of dose), which might complicate the evaluation. CYP3A5 is polymorphically expressed owing to the *CYP3A5*3* allele, causing

alternative splicing and protein truncation [43]. Surprisingly, Petros *et al.* [44] reported a reverse association, namely that the AUC of CPA was higher in patients with *CYP3A5*1* than in patients with *CYP3A5*3*. This study showed no association between the *CYP3A5*3* genotype and CPA metabolism. The contribution of GSTA1, M1, P1, and T1 isoforms to the CPA metabolism has been reported [7,45]. No polymorphisms of the *GST* genes were associated with the pharmacokinetics of 4-OH-CPA.

It has been reported that vincristine and prednisone did not affect the pharmacokinetics of CPA [46]. Besides anticancer drugs, a variety of drugs are possibly coadministered with anticancer drugs. Indeed, patients in this study received drugs such as calcium blockers, antiarrhythmic agents, antihistamines, NSAIDs, analgesics, and so on. Such many kinds of drugs, however, prohibited us to analyze the effects of comedication on the pharmacokinetics of CPA. In addition, it should be minded that we cannot interpret whether the observed myelosuppression was because of CPA or the other coadministered anticancer drugs. Thus, clinical study, especially for anticancer drugs, has several issues to be addressed.

This is the first study in which the pharmacokinetics of CPA and its metabolite and the genetic polymorphisms of drug-metabolizing enzymes were comprehensively analyzed in Japanese cancer patients. We found that SNPs in the promoter region or introns in the *CYP2B6* gene were associated with decreased CPA 4-hydroxylation and adverse reactions.

Acknowledgement

References

1 Chang TK, Weber GF, Crespi CL, Waxman DJ. Differential activation of cyclophosphamide and ifosphamide by cytochromes P-450 2B and 3A in human liver microsomes. *Cancer Res* 1993; 53:5629–5637.

2 Chang TK, Yu L, Maurel P, Waxman DJ. Enhanced cyclophosphamide and ifosfamide activation in primary human hepatocyte cultures: response to cytochrome P-450 inducers and autoinduction by oxazaphosphorines. *Cancer Res* 1997; 57:1946–1954.

3 Roy P, Yu LJ, Crespi CL, Waxman DJ. Development of a substrate-activity based approach to identify the major human liver P-450 catalysts of cyclophosphamide and ifosfamide activation based on cDNA-expressed activities and liver microsomal P-450 profiles. *Drug Metab Dispos* 1999; 27:655–666.

4 Huang Z, Roy P, Waxman DJ. Role of human liver microsomal CYP3A4 and CYP2B6 in catalyzing N-dechloroethylation of cyclophosphamide and ifosfamide. *Biochem Pharmacol* 2000; 59:961–972.

5 Fleming RA. An overview of cyclophosphamide and ifosfamide pharmacology. *Pharmacotherapy* 1997; 17:146S–154S.

6 Yu LJ, Drewes P, Gustafsson K, Brain EGC, Hecht JED, Waxman DJ. In vivo modulation of alternative pathways of P-450-catalyzed cyclophosphamide metabolism: impact on pharmacokinetics and antitumor activity. *J Pharmacol Exp Ther* 1999; 288:928–937.

7 Dirven HA, Van Ommen B, Van Bladeren PJ. Involvement of human glutathione S-transferase isoenzymes in the conjugation of cyclophosphamide metabolites with glutathione. *Cancer Res* 1994; 54:6215–6220.

8 Sladek NE. Aldehyde dehydrogenase-mediated cellular relative insensitivity to the oxazaphosphorines. *Curr Pharm Des* 1999; 5:607–625.

9 Lang T, Klein K, Fischer J, Nussler AK, Neuhaus P, Hofmann U, et al. Extensive genetic polymorphism in the human *CYP2B6* gene with impact on expression and function in human liver. *Pharmacogenetics* 2001; 11: 399–415.

10 Lamba V, Lamba J, Yasuda K, Strom S, Davila J, Hancock ML, et al. Hepatic CYP2B6 expression: gender and ethnic differences and relationship to CYP2B6 genotype and CAR (constitutive androstane receptor) expression. *J Pharmacol Exp Ther* 2003; 307:906–922.

11 Lang T, Klein K, Richter T, Zibat A, Kerb R, Eichelbaum M, et al. Multiple novel nonsynonymous CYP2B6 gene polymorphisms in Caucasians: demonstration of phenotypic null alleles. *J Pharmacol Exp Ther* 2004; 311:34–43.

12 Hesse LM, He P, Krishnaswamy S, Hao Q, Hogan K, Von Moltke LL, et al. Pharmacogenetic determinants of interindividual variability in bupropion hydroxylation by cytochrome P450 2B6 in human liver microsomes. *Pharmacogenetics* 2004; 14:225–238.

13 Klein K, Lang T, Saussele T, Barbosa-Sicard E, Schunck WH, Eichelbaum M, et al. Genetic variability of CYP2B6 in populations of African and Asian origin: allele frequencies, novel functional variants, and possible implications for anti-HIV therapy with efavirenz. *Pharmacogenet Genom* 2005; 15: 861–873.

14 Ariyoshi N, Miyazaki M, Toide K, Sawamura Y, Kamataki T. A single nucleotide polymorphism of CYP2B6 found in Japanese enhances catalytic activity by autoactivation. *Biochem Biophys Res Commun* 2001; 281:1256–1260.

15 Kirchheiner J, Klein C, Meineke I, Sasse J, Zanger UM, Murdter TE, et al. Bupropion and 4-OH-bupropion pharmacokinetics in relation to genetic polymorphisms in CYP2B6. *Pharmacogenetics* 2003; 13: 619–626.

16 Jinno H, Tanaka-Kagawa T, Ohno A, Makino Y, Matsushima E, Hanioka N, et al. Functional characterization of cytochrome P450 2B6 allelic variants. *Drug Metab Dispos* 2003; 31:398–403.

17 Xie HJ, Yasar U, Lundgren S, Griskevicius L, Terelius Y, Hassan M, Rane A. Role of polymorphic human CYP2B6 in cyclophosphamide bioactivation. *Pharmacogenomics J* 2003; 3:53–61.

18 Xie H, Griskevicius L, Stahle L, Hassan Z, Yasar U, Rane A, et al. Pharmacogenetics of cyclophosphamide in patients with hematological malignancies. *Eur J Pharm Sci* 2006; 27:54–61.

19 Timm R, Kaiser R, Lotsch J, Heider U, Sezer O, Weisz K, et al. Association of cyclophosphamide pharmacokinetics to polymorphic cytochrome P450 2C19. *Pharmacogenomics J* 2005; 5:365–373.

20 Takada K, Arefayene M, Desta Z, Yarboro CH, Boumpas DT, Balow JE, et al. Cytochrome P450 pharmacogenetics as a predictor of toxicity and clinical response to pulse cyclophosphamide in lupus nephritis. *Arthritis Rheum* 2004; 50:2202–2210.

21 Clarke L, Waxman DJ. Oxidative metabolism of cyclophosphamide: identification of the hepatic monooxygenase catalysts of drug activation. *Cancer Res* 1989; 49:2344–2350.

22 Alarcon RA. Fluorometric determination of acrolein and related compounds with m-aminophenol. *Anal Chem* 1968; 40:1704–1708.

23 Beal SL, Sheiner LB. *NONMEM user's guide*. San Francisco, California: University of California at San Francisco; 1992.

24 Xiao ZS, Goldstein JA, Xie HG, Blaisdell J, Wang W, Jiang CH, et al. Differences in the incidence of the CYP2C19 polymorphism affecting the S-mephenytoin phenotype in Chinese Han and Bai populations and identification of a new rare CYP2C19 mutant allele. *J Pharmacol Exp Ther* 1997; 281:604–609.

25 Nakajima M, Fujiki Y, Kyo S, Kanaya T, Nakamura M, Maida Y, et al. Pharmacokinetics of paclitaxel in ovarian cancer patients and genetic polymorphisms of CYP2C8, CYP3A4, and MDR1. *J Clin Pharmacol* 2005; 45:674–682.

26 Komiya Y, Tsukino H, Nakao H, Kuroda Y, Imai H, Katoh T. Human glutathione S-transferase A1 polymorphism and susceptibility to urothelial cancer in the Japanese population. *Cancer Lett* 2005; 221:55–59.

27 Vester U, Kranz B, Zimmermann S, Buscher R, Hoyer PF. The response to cyclophosphamide in steroid-sensitive nephritic syndrome is influenced by polymorphic expression of glutathione-S-transferases-M1 and -P1. *Pediatr Nephrol* 2005; 20:478–481.

28 Chen CL, Liu Q, Pui CH, Rivera GK, Sandlund JT, Ribeiro R, et al. Higher frequency of glutathione S-transferase deletions in black children with acute lymphoblastic leukemia. *Blood* 1997; 89:1701–1707.

29 Hiratsuka M, Takekuma Y, Endo N, Narahara K, Hamdy SI, Kishikawa Y, et al. Allele and genotype frequencies of CYP2B6 and CYP3A5 in the Japanese population. *Eur J Clin Pharmacol* 2002; 58:417–421.

30 Kobayashi K, Morita J, Chiba K, Wanibuchi A, Kimura M, Irie S, *et al.* Pharmacogenetic roles of CYP2C19 and CYP2B6 in the metabolism of *R-* and *S-*mephobarbital in humans. *Pharmacogenetics* 2004; 14:549–556.

31 Fukushima-Uesaka H, Saito Y, Watanabe H, Shiseki K, Saeki M, Nakamura T, *et al.* Haplotypes of CYP3A4 and their close linkage with *CYP3A5* haplotypes in a Japanese population. *Hum Mutat* 2004; 23:100 (Mutation in Brief #681).

32 Sasai Y, Horiike S, Misawa S, Kaneko H, Kobayashi M, Fujii H, *et al.* Genotype of glutathione *S-*transferase and other genetic configurations in myelodysplasia. *Leuk Res* 1999; 23:975–981.

33 Naoe T, Takeyama K, Yokozawa T, Kiyoi H, Seto M, Uike N, *et al.* Analysis of genetic polymorphism in NQO1, GST-M1, GST-T1, and CYP3A4 in 469 Japanese patients with therapy-related leukemia/myelodysplastic syndrome and de novo acute myeloid leukemia. *Clin Cancer Res* 2000; 6:4091–4095.

34 Evans WE. Pharmacogenetics of thiopurine *S-*methyltransferase and thiopurine therapy. *Ther Drug Monit* 2004; 26:186–191.

35 van Kuilenburg AB. Dihydropyrimidine dehydrogenase and the efficacy and toxicity of 5-fluorouracil. *Eur J Cancer* 2004; 40:939–950.

36 Ando Y, Hasegawa Y. Clinical pharmacogenetics of irinotecan (CPT-11). *Drug Metab Rev* 2005; 37:565–574.

37 Zukunft J, Lang T, Richter T, Hirsch-Ernst KI, Nussler AK, Klein K, *et al.* A natural *CYP2B6* TATA box polymorphism (−82T→C) leading to enhanced transcription and relocation of the transcriptional start site. *Mol Pharmacol* 2005; 67:1772–1782.

38 Desta Z, Zhao X, Shin J-G, Flockhart DA. Clinical significance of the cytochrome P450 2C19 genetic polymorphism. *Clin Pharmacokinet* 2002; 41:913–958.

39 Ren S, Yang JS, Kalhorn TF, Slattery JT. Oxidation of cyclophosphamide to 4-hydroxycyclophosphamide and deschloroethylcyclophosphamide in human liver microsomes. *Cancer Res* 1997; 57:4229–4235.

40 Griskevicius L, Yasar U, Sandberg M, Hidestrand M, Eliasson E, Tybring G, *et al.* Bioactivation of cyclophosphamide: the role of polymorphic CYP2C enzymes. *Eur J Clin Pharmacol* 2003; 59:103–109.

41 Nasu K, Kubota T, Ishizaki T. Genetic analysis of CYP2C9 polymorphisms in a Japanese population. *Pharmacogenetics* 1997; 7:405–409.

42 Murayama N, Nakamura T, Saeki M, Soyama A, Saito Y, Sai K, *et al.* CYP3A4 gene polymorphisms influence testosterone 6β-hydroxylation. *Drug Metab Pharmacokinet* 2002; 17:150–156.

43 Kuehl P, Zhang J, Lin Y, Lamba J, Assem M, Schuetz J, *et al.* Sequence diversity in *CYP3A* promoters and characterization of the genetic basis of polymorphic CYP3A5 expression. *Nat Genet* 2001; 27:383–391.

44 Petros WP, Hopkins PJ, Spruill S, Broadwater G, Vredenburgh JJ, Colvin OM, *et al.* Associations between drug metabolism genotype, chemotherapy pharmacokinetics, and overall survival in patients with breast cancer. *J Clin Oncol* 2005; 23:6117–6125.

45 DeMichele A, Aplenc R, Botbyl J, Colligan T, Wray L, Klein-Cabral M, *et al.* Drug-metabolizing enzyme polymorphisms predict clinical outcome in a node-positive breast cancer cohort. *J Clin Oncol* 2005; 23:5552–5559.

46 Bagley CM Jr, Bostick FW, DeVita VT Jr. Clinical pharmacology of cyclophosphamide. *Cancer Res* 1973; 33:226–233.

Irinotecan pharmacokinetics/pharmacodynamics and *UGT1A* genetic polymorphisms in Japanese: roles of *UGT1A1*6* and *28*

Hironobu Minami[a], Kimie Sai[b,c], Mayumi Saeki[b], Yoshiro Saito[b,d], Shogo Ozawa[b,e], Kazuhiro Suzuki[c], Nahoko Kaniwa[b,f], Jun-ichi Sawada[b,d], Tetsuya Hamaguchi[g], Noboru Yamamoto[g], Kuniaki Shirao[g], Yasuhide Yamada[g], Hironobu Ohmatsu[h], Kaoru Kubota[h], Teruhiko Yoshida[i], Atsushi Ohtsu[j] and Nagahiro Saijo[k]

Objectives SN-38, an active metabolite of irinotecan, is detoxified by glucuronidation with UGT1A isoforms, 1A1, 1A7, 1A9, and 1A10. The pharmacogenetic information on *UGT1A* haplotypes covering all these isoforms is important for the individualized therapy of irinotecan. Associations between *UGT1A* haplotypes and pharmacokinetics/ pharmacodynamics of irinotecan were investigated to identify pharmacogenetic markers.

Methods Associations between *UGT1A* haplotypes and the area under concentration curve ratio (SN-38 glucuronide/ SN-38) or toxicities were analyzed in 177 Japanese cancer patients treated with irinotecan as a single agent or in combination chemotherapy. For association analysis, diplotypes of *UGT1A* gene segments [(*1A1, 1A7, 1A9, 1A10*), and Block C (common exons 2–5)] and combinatorial haplotypes (*1A9-1A7-1A1*) were used. The relationship between diplotypes and toxicities was investigated in 55 patients treated with irinotecan as a single agent.

Results Among diplotypes of *UGT1A* genes, patients with the haplotypes harboring *UGT1A1*6* or *28* had significantly reduced area under concentration curve ratios, with the effects of *UGT1A1*6* or *28* being of a similar scale. A gene dose effect on the area under concentration curve ratio was observed for the number of haplotypes containing *28* or *6* (5.55, 3.62, and 2.07 for 0, 1, and 2 haplotypes, respectively, *P* < 0.0001). In multivariate analysis, the homozygotes and double heterozygotes of *6* and *28* (*6/*6, *28/*28 and *6/*28) were significantly associated with severe neutropenia in 53 patients who received irinotecan monotherapy.

Conclusions The haplotypes significantly associated with reduced area under concentration curve ratios and neutropenia contained *UGT1A1*6* or *28*, and both of them should be genotyped before irinotecan is given to Japanese and probably other Asian patients. *Pharmacogenetics and Genomics* 17:497–504 © 2007 Lippincott Williams & Wilkins.

[a]Division of Oncology/Hematology, National Cancer Center Hospital East, Kashiwa, [b]Project Team for Pharmacogenetics, [c]Division of Biosignaling, [d]Division of Biochemistry and Immunochemistry, [e]Division of Pharmacology, [f]Division of Medicinal Safety Science, National Institute of Health Sciences, [g]Division of Internal Medicine, National Cancer Center Hospital, [h]Division of Thoracic Oncology, National Cancer Center Hospital East, Kashiwa, [i]Genetics Division, National Cancer Center Research Institute, Tokyo, [j]Division of Gastrointestinal Oncology/Digestive Endoscopy and [k]National Cancer Center Hospital East, Kashiwa, Japan.

Correspondence to Hironobu Minami, MD, Head and Chair, Division of Oncology/Hematology, National Cancer Center Hospital East, 6-5-1 Kashiwanoha, Kashiwa 277-8577, Japan
Tel: +81471331111; e-mail: hminami@east.ncc.go.jp

Introduction

Irinotecan, an anticancer prodrug, is widely applied for colorectal, lung, stomach, ovarian, and other various cancers. It is activated by carboxylesterases to SN-38 (7-ethyl-10-hydroxycamptothecin), which shows antitumor activity by inhibiting topoisomerase I [1,2]. SN-38 is subsequently glucuronidated by uridine diphosphate glucuronosyltransferases (*UGTs*) to form an inactive metabolite, SN-38 glucuronide (SN-38G) [3]. Dose-limiting toxicities of irinotecan are diarrhea and leukopenia [4], and reduced activity for SN-38G formation is closely related to severe toxicities [5]. Among UGT

isoforms, UGT1A1 is abundant in both the liver and intestine and is thought to be mainly responsible for inactivation of SN-38 [3,6]. Genetic polymorphisms of *UGT1A1* result in reduced enzyme activity and increased toxicity by irinotecan. A significant association of *UGT 1A1*28*, a repeat polymorphism of the TATA box (-40_-39insTA) [3,7], with severe irinotecan-induced diarrhea/leukopenia was first reported in a retrospective study of Japanese cancer patients [8]. Subsequent pharmacogenetic studies in Caucasians have shown close associations of *28* with reduced glucuronidation of SN-38 and/or severe neutropenia/diarrhea [9–12]. These

studies have clearly indicated that *28 is a good genetic marker for individualized irinotecan therapy. On the basis of these observations, the Food and Drug Administration of the United States has approved an amendment of the label for Camptosar (irinotecan HCl) and added a warning to consider a reduction in the starting dose of irinotecan for *28 homozygous patients (NDA 20-571/S-024/S-027/S-028).

There is significant racial difference in UGT1A1 polymorphisms among Asians, Caucasians, and Africans [13]. Although the association of UGT 1A1*28 with toxicities by irinotecan was first described in Japanese patients, its frequency in Japanese is one-third of that in Caucasians. Another low-activity allele *6 [211G >A(G71R)], which is not detected in Caucasians or Africans, is as frequent as the *28 allele in Japanese. Moreover, the area under concentration curve (AUC) ratio of SN-38G to SN-38 was decreased in patients having *6 haplotypes [14].

In addition to UGT1A1, recent studies have suggested possible contributions to SN-38G formation by UGT1A7, 1A9, and 1A10 [15–17], which are expressed in the gastrointestinal tract, the liver and intestine, and extrahepatic tissues, respectively [18]. Altered activity resulted from genetic polymorphisms of these isoforms, including 1A7*3 [387T > G(N129K), 391C > A(R131K), 622T >C(W208R)], 1A9*22 (-126_-118T$_9$ > T$_{10}$), 1A9*5 [766G >A(D256N)], and UGT1A10*3 [605C > T(T202I)], but clinical relevance of these polymorphisms is yet to be elucidated [16,19–24]. Moreover, close linkages among 1A9, 1A7, and 1A1 polymorphisms were found in Caucasians and Asians in an ethnic-specific manner [20,25–27]. Therefore, comprehensive investigation that covers these genes, along with linkages among the polymorphisms, is needed, in each ethnic population, to evaluate associations between the genetic polymorphisms and pharmacokinetics, as well as clinical outcomes of irinotecan therapy.

Recently, we have analyzed the segmental and block haplotypes of 1A8, 1A10, 1A9, 1A7, 1A6, 1A4, 1A3 and 1A1, and the common exons 2–5 (Block C) in a Japanese population, including the 177 cancer patients treated with irinotecan, and showed close linkages between the haplotypes, that is, 1A9*22 and 1A7*1, 1A7*3 and 1A1*6, and 1A7*3 and 1A1*28 [28]. Preliminary results of UGT1A1 pharmacogenetics on 85 of these cancer patients were reported previously [14]. In the current study, we investigated the pharmacogenetics of irinotecan, focusing on diplotypes of the UGT1A complex covering 1A1, 1A7, 1A9, 1A10, and Block C (exons 2–5) of 177 patients, so as to elucidate haplotypes or genetic markers associated with altered glucuronidation of SN-38 and toxicities.

Methods
Patients and treatment schedule
Patients with cancers who started chemotherapy with irinotecan at two National Cancer Center Hospitals

(Tokyo and Kashiwa, Japan) were eligible if they had not received irinotecan previously. Other eligibility criteria included bilirubin ≤ 2 mg/dl, aspartate aminotransferase (GOT) ≤ 105 IU/l, alanine aminotransferase (GPT) ≤ 120 IU/l, creatinine ≤ 1.5 mg/dl, white blood cell count ≥ 3000/μl, performance status of 0–2, and at least 4 weeks after the last chemotherapy (2 weeks for radiotherapy). Exclusion criteria were diarrhea, active infection, intestinal paralysis or obstruction, and interstitial pneumonitis. The ethics committees of the National Cancer Center and the National Institute of Health Sciences approved this study, and written informed consent was obtained from all participants.

Irinotecan was administered as a single agent or in combination chemotherapy at the discretion of attending physicians. Doses and schedules were according to approved usage in Japan; intravenous 90-min infusion at a dose of 100 mg/m^2 weekly or 150 mg/m^2 biweekly. In terms of combination chemotherapy, the dose of irinotecan was reduced according to clinical protocols.

Genetic polymorphisms of UGT1As and pharmacokinetics
Detailed assay methods for genotypes of the UGT1A gene complex were reported previously [14,28]. In this study, we focused on the genetic variations in UGT1A1, 1A7, 1A9, and 1A10 and common exons 2–5, as they have been reported to contribute to the SN-38 glucuronidation. Haplotype analysis covering these regions was performed in our previous study [28], and haplotypes of each UGT1A segment [exon 1 for 1A1, 1A7, 1A9, or 1A10; and Block C (common exons 2–5)] are summarized in Fig. 1.

Pharmacokinetic analysis for irinotecan was performed as described previously [14]. Briefly, heparinized blood was collected before administration of irinotecan, as well as 0 and 20 min, and 1, 2, 4, 8, and 24 h after termination of the first infusion of irinotecan. Plasma concentrations of irinotecan, SN-38 and SN-38G were determined by the high-performance liquid chromatography [29], and AUC was calculated by the trapezoidal method using WinNonlin version 4.01 (Pharsight Corporation, Mountain View, California, USA). Associations between genotypes and the AUC ratio (AUC of SN-38G/AUC of SN-38) were evaluated in 176 patients.

Monitoring and toxicities
A complete medical history and data on physical examinations were recorded before the irinotecan therapy. Complete blood cell counts with differentials and platelet counts, as well as blood chemistry, were measured once a week during the first 2 months of irinotecan treatment. Toxicities were graded according to the Common Toxicity Criteria of National Cancer Institute version 2. Association of genetic factors with irinotecan toxicities was analyzed primarily in patients who received irinotecan as a single agent.

Fig. 1

UGT1A1

Region	Enhancer	Promoter	Exon 1		Frequency
Nucleotide change	-3279 T>G	-40_-39 insTA	211 G>A	686 C>A	
Amino acid change			G71R	P229Q	
Marker allele	*60	*28	*6	*27	

Haplotype						Frequency
*1						0.548
*6						0.167
*60						0.147
*28	*28b					0.138
	*28c					
	*28d					

UGT1A10

Region	Exon 1				Frequency
Nucleotide change	4 G>A	177 G>A	200 A>G	605 C>T	
Amino acid change	A2T	M59I	E67G	T202I	
Marker allele	*2T	*2	*67G	*3	

Haplotype					Frequency
*1					0.981
*2					0.006
*2T					0.003
*3					0.010
*67G					0.000

UGT1A7

Region	Exon 1				Frequency
Nucleotide change	387 T>G	391C>A	392 G>A	622 T>C	
Amino acid change	N129K	R131K		W208R	
Marker allele	*2,*3	*2,*3	*2,*3	*3,*4	

Haplotype					Frequency
*1					0.630
*2					0.147
*3					0.223

Block C

Region	Exon.4	Exon.5		3'-UTR			Frequency
Nucleotide change	1091 C>T	1456 T>G	1598 A>C	*211(1813) C>T	*339(1941) C>G	*440(2042) C>G	
Amino acid change	P364L	Y486D	H533P				
Marker allele	*364L	*7	*533P	*IB	*IB	*IB	

Haplotypes								Frequency
*IA								0.864
*IB	*1b-*1j							0.127
	*533P							
*7								0.003
*364L								0.006

UGT1A9

Region	Promoter		Exon1			Frequency
Nucleotide change	-126_-118 T9>T10	-126_-118 T9>T11	422 C>G	726 T>G	766 G>A	
Amino acid change			S141C	Y242X	D256N	
Marker allele	*22	*T11	*141C	*4	*5	

Haplotype						Frequency
*1						0.347
*22						0.644
*141C						0.000
*4						0.000
*5						0.006
*T11						0.003

Haplotypes of UGT1A gene segments (UGT1A1, 1A7, 1A9, 1A10, and Block C) in 177 Japanese cancer patients. The tagging variations and haplotypes are shown. Variant alleles are indicated in grey. Definition of Block C haplotypes in our previous paper ([14]) (corresponding to Block 2) were slightly modified.

Statistical analysis

Statistical analysis on the differences in the AUC ratios (SN-38G/SN-38) among UGT1A genotypes was performed using the Kruskal–Wallis test, followed by nonparametric Dunnett's multiple comparison test, or with Wilcoxon test. Analysis of a gene–dose effect of each haplotype was performed using the Jonckheere–Terpestra test in the SAS system, version 5.0 (SAS Institute, Cary, North Carolina, USA). Relationship of UGT1A genetic polymorphisms to the toxicities of irinotecan was assessed by the χ^2 test via the use of using Prism version 4.0 (GraphPad Prism Software, San Diego, California, USA). The P-value of 0.05 (two-tailed) was set as a significant level, and the

multiplicity adjustment was conducted for pharmacokinetics data with the false discovery rate [30].

To identify factors associated with the log-transformed AUC ratio of SN-38G/SN-38, multiple regression analysis was performed using age, sex, body surface area, dosage of irinotecan, history of smoking or drinking, performance status, coadministered drugs, serum biochemistry parameters at baseline, and 1A9-1A7-1A1 and Block C haplotypes (five or more chromosome numbers) or '1A1*6 or *28'. For multiple regression analysis of neutropenia, variables included the absolute neutrophil count at baseline and the dosing interval, in addition to

the other patient background factors described above. The multivariate analyses were performed by using JMP version 6.0.0 software (SAS Institute). The variables in the final models for both AUC ratio and neutropenia were chosen by forward and backward stepwise procedures at significance levels of 0.25 and 0.05, respectively.

Results

Patients and UGT1A haplotypes

Patient demographics and information on the treatment are summarized in Table 1. In addition to UGT1A1, UGT1A7, 1A9, and 1A10 were also reported to glucuronidate SN-38 [15–17]. In our previous study, haplotype analysis covering the 1A9 to 1A1 (5'–3') gene segments was conducted, and the combinatorial diplotypes (1A9-1A7-1A1) of the patients were determined. It must be noted that close linkages between 1A9*22 and 1A7*1, between 1A7*2 and 1A1*60, and between 1A7*3 and 1A1*6 or 1A1*28 were observed as described previously [28]. To clarify the linkages between these segmental haplotypes (1A9, 1A7, and 1A1), we grouped the combinatorial (1A9-1A7-1A1) haplotypes into four categories (A–D) based on the 1A1 haplotypes (*1, *6, *60, and *28). Each group was further divided into the subgroups based on the previously defined Block 9/6 (including 1A9, 1A7, and 1A6) haplotypes (Table 2). The frequency of Group B haplotypes (B1-B4) harboring 1A1*6 was 0.167 and higher than that of Group D haplotypes (D1-D6) with *28 (0.138) in this population.

Association of 1A9-1A7-1A1 diplotypes to SN-38G formation

When relationship between the UGT1A diplotypes (1A9-1A7-1A1) and the SN-38G/SN-38 AUC ratio was analyzed

in the 176 cancer patients the AUC ratio for the diplotypes of B2/B2, D2/A1, and D1/B2 was statistically significantly lower than the A1/A1 diplotype (Fig. 2). These diplotypes harbored 1A1*6, *28 or both. Significant gene–dose effects of B2 (among A1/A1, B2/A1, and B2/B2) and C3 (among A1/A1, C3/A1, and C3/C3) were also observed (Fig. 2). As no significant differences in AUC ratios were observed between D1/A1 and D2/A1, D1/C3 and D2/C3, and D1/B2 and D2/B2, the haplotype combination 1A9*1-1A7*3 or 1A9*22-1A7*1 was not influential on the AUC ratio.

As the effect of diplotypes harboring UGT1A1 polymorphism was prominent, we grouped the whole gene (1A9-1A7-1A1) diplotypes according to the 1A1 diplotypes (the upper part of Fig. 2). Patients with *6 or *28 (except for *28/*28) haplotypes had significantly lower AUC ratios than the wild-type (*1/*1), and significant gene–dose effects were observed for *28 (among *1/*1, *28/*1, and *28/*28) and *6 (among *1/*1, *6/*1 and *6/*6). A significant additive effect of *6 and *28 on the decreased AUC ratio was also observed when the values for *28/*1 were compared with those for *28/*6 (Fig. 2 and Table 3).

Regarding other polymorphisms, a statistically nonsignificant tendency to decrease the AUC ratio was observed for *60

Table 1 Characteristics of Japanese cancer patients in this study

		No. of participants	
Age			
Mean/range	60.5/26–78	177	
Sex			
Male/female		135/42	
Performance status	0/1/2	84/89/4	
Combination therapy and tumor type			
(initial dose of irinotecan; mg/m²)			
Irinotecan monotherapy	Lung (100)	21	
	Colon (150)	28	
	Others (100)	7	
With platinum-containing	Lung (60)	58[b]	48 [60][c]
drug[a]	Stomach (70)	9	9 [80][c]
	Others (60)	5	5 [80][c]
With 5-fluorouracil	Colon (100 or 150)	34	
(including tegafur)	Others (90 or 100)	2	
With mitomycin-C	Stomach (150)	10	
	Colon (150)	1	
With amrubicin	Lung (60)	2	
Previous treatment			
Surgery	Yes/no	85/92	
Chemotherapy	Yes/no	97/80	
Radiotherapy	Yes/no	26/151	
Smoking history	Yes/no	29/148	

[a]Cisplatin, cisplatin plus etoposide or carboplatta.
[b]Two and eight patients received cisplatin and etoposide and carboplatin, respectively.
[c]Number of cisplatin-administered patients [initial dose of cinlatin (mg/m²) is shown in brackets].

Table 2 Combinatorial haplotypes covering UGT1A9, UGT1A7, and UGT1A1

Haplotype	Block haplotype[a]			Combination of segmental haplotypes 1A9-1A7-1A1	Cancer patients	
	Block 9/6	Block 4	Block 3/1		N[b]	Frequency
A1[c]	*1	*1	*1	*22-*1-*1	189	0.534
	*1	*3	*1			
A3	*III	*1	*1	*1-*2-*1	2	0.006
A2	*II	*1	*1	*1-*3-*1	1	0.003
A4	*IV	*1	*1	*22-*3-*1	1	0.003
A5				*T11-*1-*1	1	0.003
B2[c]	*II	*1	*III			
	*II	*1	*VI	*1-*3-*6	47	0.133
	*II	*4	*VI			
B4	*IV	*1	*III	*22-*3-*6	6	0.017
B1	*1	*1	*III	*22-*1-*6	5	0.014
	*1	*1	*VI			
B3	*III	*1	*III	*1-*2-*6	1	0.003
C3[c]	*III	*3	*IV			
	*III	*1	*IV			
	*III	*3	*V	*1-*2-*60	44	0.124
	*III	*1	*V			
C1	*1	*3	*IV	*22-*1-*60	5	0.014
	*1	*1	*IV			
C2	*II	*3	*IV	*1-*3-*60	2	0.006
C7	*VII	*3	*V	*22-*2-*60	1	0.003
D1	*1	*1	*IIa	*22-*1-*28	23	0.065
	*1	*1	*IIc			
D2	*II	*1	*IIa			
	*II	*3	*IIa	*1-*3-*28	22	0.062
	*II	*1	*IIc			
D6	*VI	*1	*IIb	*1-*2-*28	4	0.011
				Total	354	1.000

[a]Block haplotypes described in Ref. [28] are shown for reference. 1A9 and 1A7 are included in block 9/6 and 1A1 is included in block 3/1.
[b]Number of chromosomes.
[c]Major combinatrial haplotypes.

Fig. 2
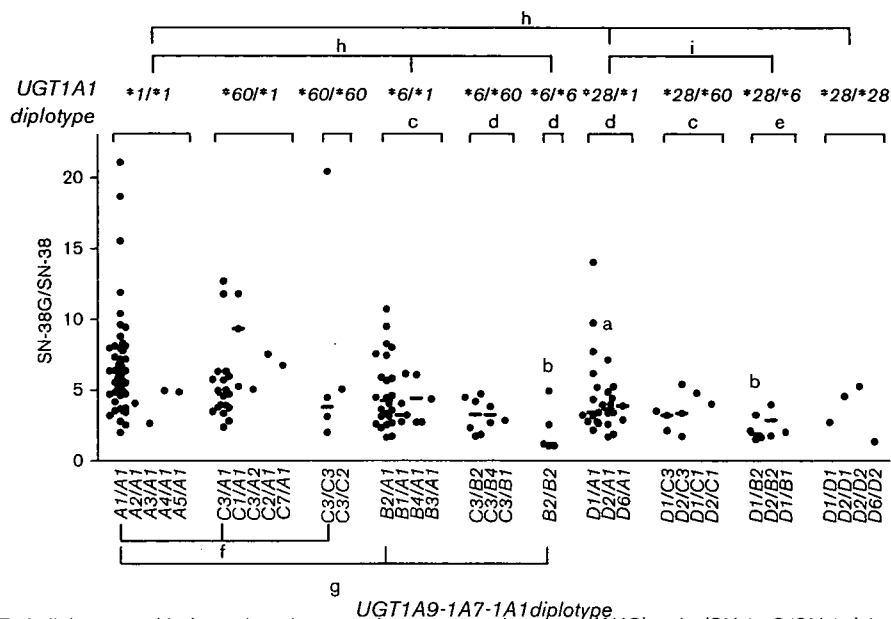
The association of *UGT1A* diplotypes with the reduced area under concentration curve (AUC) ratio (SN-38G/SN-38) in 176 Japanese cancer patients who received irinotecan. The whole gene (*1A9-1A7-1A1*) diplotypes are shown below the abscissa and the *UGT1A1* diplotypes are indicated in the upper part of the figure. Each point represents a patient value, and the median is indicated by a bar. Significant reductions in the AUC ratio were detected in the *B2/B2*, *D2/A1*, and *D1/B2* compared with *A1/A1* for the whole gene diplotypes [Kruskal–Wallis test (*P*=0.0009) followed by Dunnett's multiple comparison test]. As for the *1A1* diplotypes, significant reductions were detected in the *6/*1*, *6/*60*, *6/*6*, *28/*1*, *28/*60*, and *28/*6* compared with the *1/*1* group [Kruskal–Wallis test (*P*<0.0001) followed by Dunnett's multiple comparison test]. Gene–dose effects on the reduced AUC ratio were significant for *6* and *28* (Jonckheere–Terpestra test). A significant additive effect of *6* on the reduced AUC ratio by *28* was detected by comparing *28/*1* and *28/*6*. [a]$P<0.05$ and [b]$P<0.01$ against *A1/A1* group (Dunnett's multiple comparison test); [c]$P<0.05$, [d]$P<0.01$, and [e]P&<0.001 against the *1/*1* group (Dunnett's multiple comparison test); [f]$P<0.05$, [g]$P<0.001$, and [h]$P<0.0001$ (Jonckheere–Terpestra test for gene–dose effect); [i]$P<0.01$ (Wilcoxon test).

(*P* = 0.1134). No significant effects on the AUC ratio were observed for Block C (exon 2–5) haplotypes or rare variations including *1A10* (*2T*, *2*, or *3*) and *1A9* (*5*, *T11*).

Multiple regression analysis of the area under concentration curve ratio

We further assessed the impact of *UGT1A* genetic factors on the AUC ratio by multiple regression analysis. First, we used the *1A9-1A7-1A1* and Block C haplotypes as genetic factors. The AUC ratio was significantly associated with the haplotypes *B2*, *D1*, and *D2* and serum biochemistry parameters indicating hepatic or renal function before treatment. The Groups B and D haplotypes harbor *1A1*6* and *28*, respectively. The dependency on specific *1A7* or *1A9* polymorphisms, however, was not obtained, considering the contributions of both *D1* and *D2*. As *1A1*6* and *28* are mutually exclusive and their effects are comparable, we grouped *1A1*6* and *28* into the same category in the final multiple regression model (Table 4). The final model confirmed the significant contribution of this genetic marker (*6* or *28*) to the AUC ratio.

Effects of the genetic marker '*6 or *28' on pharmaco kinetic parameters

Then, a dose effect of the genetic marker '*6 or *28' on pharmacokinetic parameters was further analyzed

Table 3 AUC ratio of SN-38 glucuronide to SN-38 for *UGT1A1* diplotypes

| Diplotype | Number of patients | AUC ratio | | *P*-value[a] (vs. *1/*1) |
		Median	Interquartile range	
*1/*1	55	6.13	4.72–7.79	
*1/*60	25	5.04	3.85–6.52	0.9803
*60/*60	5	4.48	2.57–12.74	0.8141
*6/*1	32	4.03	2.74–5.97	0.0126
*6/*60	9	2.84	2.09–4.33	0.0021
*6/*6	5	1.19	1.06–3.74	0.0012
*28/*1	26	3.65	2.76–5.21	0.0040
*28/*60	8	3.44	2.68–4.40	0.0261
*28/*6	7	2.03	1.65–3.26	<0.0001
*28/*28	4	3.65	2.05–4.92	0.2322

AUC, area under concentration curve.
[a]Dunnett's multiple comparison test.

(Fig. 3). Patients with one haplotype harboring either *6 or *28 (*6/*1, *6/*60, *28/*1, and *28/*60) had lower SN-38G/SN-38 AUC ratios (median, 3.62; interquartile range, 2.74–5.18) than patients without *6 or *28 (*1/*1, *60/*1, and *60/*60) (5.55, 4.13–7.26), and patients with two haplotypes harboring *6 or *28 (*6/*6, *28/*28, and *28/*6) had the lowest AUC ratio (2.07, 1.45–3.62) (*P* < 0.0001, Fig. 3a). Similarly, the number of the *6 or *28-containing haplotypes affected the AUC ratios of SN-38 to irinotecan (Fig. 3b). When the correlations

between irinotecan dosage and the AUC of SN-38 were tested, different correlations were obtained according to the number of the haplotypes (Fig. 3c). The slope of regression line for one and two haplotypes harboring *6 or *28 was 1.4-fold and 2.4-fold greater, respectively, than that for the diplotype without *6 or *28.

Associations of UGT1A1 genetic polymorphisms with toxicities

Association between genetic polymorphisms and toxicities was investigated in patients receiving irinotecan as a single agent. One patient was referred to another hospital 3 days after the first administration of irinotecan without evaluating toxicities and was lost in terms of follow-up. Therefore, association between genetic polymorphisms and toxicities was investigated in 55 patients. Six (11%) and 14 (25%) patients experienced grade 3 or greater diarrhea and neutropenia, respectively. As for the 1A9-1A7-1A1 diplotypes, a higher incidence of grade 3 or greater neutropenia was observed in D1/B2 (1A1*28/*6) (100%, n = 3) than in A1/A1 (11.8%, n = 17) (P = 0.0088, Fisher's exact test), indicating clinical impact of the genetic marker 1A1*6 or *28. As for the dose effect of '*6 or *28', incidences of grade 3 or 4 neutropenia were 14, 24, and 80% for 0, 1, and 2 haplotypes harboring these markers, respectively (Table 5). A significant association between '*6 or *28'and neutropenia was also observed for 62 patients who received irinotecan in combination with cisplatin (Table 5). No association, however, was observed between diarrhea and the marker '*6 or *28'.

Multivariate analysis for irinotecan toxicities

We further evaluated the effect of the genetic marker '*6 or *28' on neutropenia in multivariate analysis, and confirmed a significant correlation of '*6 or *28' with the nadir of absolute neutrophil counts (Table 6). Elevated alkaline phosphatase levels and the absolute neutrophil count at baseline were also significant.

Discussion

The association study with the 1A9-1A7-1A1 diplotypes revealed that the reduction in inactivation of SN-38, as well

Table 4   Multiple regression analysis toward the AUC ratio (SN-38G/SN-38)[a]

Variable	Coefficient	F-value	P-value	R^2	Intercept	N
				0.410	0.8869	176
*6 or *28	-0.189	70.2	<0.0001			
Age	0.005	8.88	0.0033			
Serum albumin level[b]	-0.136	9.92	0.0019			
Serum GOT and ALP[c]	0.070	8.88	0.0033			
Serum creatinine[d]	0.210	7.23	0.0079			

ALP, alkaline phosphatase; AUC, area under concentration curve.
[a]The values after logarithmic conversion were used as an objective variable.
[b]The absolute value (g/dl) before irinotecan treatment.
[c]Grade 1 or greater scores in both serum GOT and ALP before irinotecan treatment.
[d]Grade 1 or greater scores in serum creatinine before irinotecan treatment.

as neutropenia, was dependent on the Groups B and D haplotypes which corresponded to the 1A1*6 and *28 segmental haplotypes. Also, multivariate analyses clearly showed clinical significance of the genetic marker '*6 or *28' for both pharmacokinetics and toxicity of irinotecan in Japanese patients (Tables 3 and 6). UGT1A1*6 and *28 were mutually exclusive [14] and contributed to the reduction in glucuronidation of SN-38 to the same extent. Therefore, the activity of SN-38 glucuronidation in individuals depended on the number of the haplotypes harboring *6 or *28. Although the role of 1A1*28 for irinotecan toxicity has been focused on [8–12], this study strongly suggests that *6 should be tested in addition to *28 before starting chemotherapy with irinotecan in Japanese patients.

The clinical importance of *6 for neutropenia by irinotecan was also supported by a recent report in Korean patients who received irinotecan and cisplatin [31]. Although no patients with irinotecan as a single agent were homozygous for *6 in our study, clinical significance of the double heterozygote, *6/*28, was clearly demonstrated. Among patients treated with irinotecan in combination chemotherapy, the majority of patients received platinum agents in our study. A significant association of '*6 or *28' with a higher incidence of grade 3 or 4 neutropenia was also observed in patients who received irinotecan and cisplatin (Table 5). These findings further support the necessity of testing '*6 or *28' before irinotecan is given to patients.

As possible enhancement of toxicities by the *27 allele was suggested [8], we evaluated the effect of the *28c haplotype, which had an additional single-nucleotide polymorphism [*27; 686C > A(P229Q)] to the *28 allele (-40_-39insTA). In our cohort of patients, there were three *28c heterozygotes (*28c/*1) and one double heterozygote (*28b/*28c). The values of the AUC ratio were within the range of variations of the *28 group, and no additional impact of *28c was observed in relation to toxicities.

Although the decreasing trend of the AUC ratio for 1A1*60 (and combinatorial haplotype C3) was observed (Fig. 2), the contribution of 1A1*60 to toxicities was not clearly demonstrated in this study as reported in the Japanese retrospective study [32].

In addition to UGT1A1, recent studies have suggested possible contributions of UGT1A7, 1A9, and 1A10 to SN-38G formation [15–17]. An in-vitro study demonstrated that 1A7*3 [387T > G(N129K), 391C > A(R131K), 622T > C(W208R)] had reduced activity in terms of SN-38G formation [16]. Results of clinical studies, however, on the association between 1A7 polymorphisms and irinotecan toxicity/efficacy are inconsistent, whereas different populations with different combination therapies were used [19,20]. Furthermore, it was reported that the UGT1A7 polymorphisms (*2 and *3), which were linked to 1A9*1, were associated with a lowered incidence